

# Carbon Cycle Extremes Accelerate Weakening of the Land Carbon Sink in the Late 21st Century

Bharat Sharma<sup>1,2</sup>, Jitendra Kumar<sup>3</sup>, Auroop R. Ganguly<sup>1</sup>, and Forrest M. Hoffman<sup>2,4</sup>

<sup>1</sup>Sustainability and Data Sciences Laboratory, Department of Civil and Environmental Engineering, Northeastern University, Boston, Massachusetts, USA

<sup>2</sup>Computational Sciences & Engineering Division and the Climate Change Science Institute, Oak Ridge National Laboratory, Oak Ridge, Tennessee, USA

<sup>3</sup>Environmental Sciences Division, Oak Ridge National Laboratory, Oak Ridge, Tennessee, USA

<sup>4</sup>Department of Civil and Environmental Engineering, University of Tennessee, Knoxville, Tennessee, USA

**Correspondence:** Bharat Sharma (bharat.sharma.neu@gmail.com)

**Abstract.** Rising atmospheric CO<sub>2</sub> concentrations enhance vegetation growth through increased carbon fertilization and water-use efficiency. Terrestrial vegetation takes up more than one-quarter of global anthropogenic carbon emissions and is modulated by regional climate. Increasing surface temperature could lead to enhanced evaporation, reduced soil moisture availability, and more frequent droughts and heatwaves. The spatio-temporal co-occurrence of such effects further drives extreme anomalies

5 in vegetation productivity and net land carbon storage. However, impacts of climate change on extremes in net biome productivity (NBP) over longer time periods are unknown. Here we show that due to climate warming, about 70% of the regions will experience a growing number of negative extremes in NBP than positive NBP extremes toward the end of 2100, which accelerate weakening of the land carbon sink. While the most dominant climate driver of NBP extremes is soil moisture, 50% of the total grid cells affected by NBP extremes are impacted by the compound effect of hot, dry, and fire. In high latitudes, 10 the positive feedback of temperature and NBP weakens toward the end of the 21st century as the frequency of co-occurrences of high temperatures and negative NBP extremes increases. Our analysis indicates the frequency of extremes associated with declines in biome productivity is larger than with gains, especially in tropics. The larger proportion of negative NBP extremes raises a concern about whether the Earth is capable of increasing vegetation production with growing human population and rising demand of plant material for food, fiber, fuel, and building materials. The rising proportion of negative NBP extremes 15 highlights the consequences of not only reduction in total carbon uptake capacity but also of conversion of land to a carbon source.

## Short summary

Rising atmospheric CO<sub>2</sub> enhances the vegetation growth through increased carbon fertilization and water-use efficiency. The increasing surface temperature driven by CO<sub>2</sub> of Earth could lead to enhanced evaporation, reduction in available soil moisture, 20 and increases in droughts and heatwaves. The impact of such climate extremes is detrimental to the terrestrial carbon uptake capacity. We investigated the extremes events in net biomass productivity (NBP), a component of the terrestrial carbon cycle

and a measure of net carbon storage flux. We found that due to climate warming about 70% of the regions towards the end of 2100 will show anomalous losses in biome productivity than gains. While lack of soil moisture alone causes the largest number of losses in biome productivity, the compound effect of hot, dry, and fire events drivers 50% of all NBP extremes. A few high 25 latitudinal regions that were net carbon sinks during warm months are expect to show negative temperature sensitivity to NBP over time. This increased number of negative NBP extremes raises a concern about whether the Earth is capable of increasing its capacity to increase vegetation production with increasing human population and rising plant material per capita demand for food, fiber, fuel, and building material.

## 1 Introduction

30 The rising anthropogenic carbon emissions ( $\text{CO}_2$ ) are leading to increase in Earth's surface temperature, climate variability and intensification of climate extremes. Terrestrial ecosystems have historically taken up a little over one-quarter of total carbon emissions, via carbon accumulation in forest biomass and soils (Friedlingstein et al., 2019), and helped constrain increasing atmospheric  $\text{CO}_2$  concentrations. The increase in net terrestrial carbon sink is a result of decline in deforestation, enhanced vegetation growth driven by  $\text{CO}_2$  fertilization and lengthening of growing seasons in high latitudes. The terrestrial carbon sink 35 provides negative feedback in the climate-carbon cycle. However, exacerbated environmental changes and climate extremes such as droughts, heatwaves and fires have the potential to reduce regional carbon stocks and carbon uptake (Reichstein et al., 2013; Sharma et al., 2022). Net biome production (NBP), one of the components of terrestrial carbon cycle, represents the net carbon uptake after accounting for carbon losses from plant respiration, autotrophic respiration, fire, and harvest (Bonan, 2015) and is a critical measure of long-term carbon storage. Climate driven large anomalies in NBP could impact the structure, 40 composition, and function of terrestrial ecosystems (Frank et al., 2015). To improve our understanding of the climate-carbon feedback, especially during large anomalies, it is important to investigate the changing magnitude, frequency, and spatial distribution of NBP extremes over long periods and identify the climate drivers at regional and global scales that potentially drive the large NBP extremes.

The terrestrial carbon cycle processes, such as photosynthesis, respiration and elemental cycling drive the structure, com- 45 position and function of the terrestrial ecosystems. In the past few decades, the global terrestrial carbon cycle has taken up 25-35 % of the  $\text{CO}_2$  emissions from anthropogenic activities such as deforestation and fossil fuel consumption (Piao et al., 2019). With rising atmospheric carbon dioxide, the carbon uptake by both ocean and land has also increased but with significant variability over land (Friedlingstein et al., 2019). Since 1980, large interannual variation in the atmospheric  $\text{CO}_2$  growth 50 rate and land carbon are correlated and driven by large-extent climate extremes and lower carbon sequestration (Piao et al., 2019).

The climate extremes are part of Earth's climatic variability affecting terrestrial vegetation and modifying ecosystem-atmosphere feedback (von Buttlar et al., 2018). A number of recent studies have investigated the influence of global warming on climate extremes and terrestrial ecosystem (von Buttlar et al., 2018; Diffenbaugh et al., 2017; Frank et al., 2015; Zscheischler et al., 2018; Sharma et al., 2022). The observations and climate models suggest that global warming has increased the

55 severity and occurrence of hottest month, hottest day, driest and wettest periods (Diffenbaugh et al., 2017). Heavy precipitation or lack thereof could have negative feedback on the carbon cycle via soil water-logging and drought stress, respectively (Reichstein et al., 2013). A few studies have investigated the impact of climate extremes on the carbon cycle and found that hot and dry extremes reduce the carbon uptake, especially in low latitudes and arid/semi-arid regions (Pan et al., 2019; Frank et al., 2015). The attribution studies infer that the compound effect of multiple climate drivers have a larger effect on carbon cycle  
60 and extremes (Sharma et al., 2022; Zscheischler et al., 2018; Pan et al., 2019; Frank et al., 2015; Reichstein et al., 2013) than any individual climate driver. Most attribution methods focus on analyzing response of carbon cycle to climate, aggregated over annual, sub-annual, and seasonal scales, however, the responses may vary at shorter time scales of daily to monthly.

The variability in climate-carbon feedbacks is dependent on geographical location, among other factors. Grose et al. (2020) reported that while Australia is expected to experience an overall reduction in precipitation by 2100, spatial distribution varies  
65 as a few regions are expected to get higher and others will receive less precipitation. Ault (2020) found that despite the overall increase in precipitation and water use efficiency globally, the available soil moisture is reducing across many regions due to increased evapotranspiration from higher temperature exceeding the supply from precipitation. The regions that see a decrease in supply and increase in demand for water are sensitive to even low levels of rising temperatures. These feedbacks will increase the severity of droughts and ENSOs will further amplify the effect (Ault, 2020). The net primary productivity (NPP) sensitivity  
70 to temperature is negative above 15°C and positive below 10°C (Pan et al., 2019), which means warming will cause a reduction in carbon uptake in tropics and extra-tropics and an increase in carbon uptake at higher latitudes. However, with increasing average surface temperatures, the NPP sensitivity could turn negative over time in high latitude regions.

The rising CO<sub>2</sub> and global warming could have implications for biological (Frank et al., 2015) and ecological systems as the severity and occurrence of climate extremes, such as heatwaves, droughts, and fires, are likely to strengthen in the future. These  
75 systems are more sensitive to climate and carbon extremes than gradual climate change. Increasing frequency and magnitude of climate extremes could lead to reduction in carbon uptake in tropical vegetation, reduce crop yield (Ribeiro et al., 2020), and negate the expected increase in carbon uptake (Reichstein et al., 2013). In this study we investigated the extremes in the NBP and their climate drivers during 1850 – 2100 across several regions around the globe. The objectives of this study were 1)  
80 to quantify the magnitude, frequency, and spatial distribution of NBP extremes, 2) attribute individual and compound climate drivers of NBP extremes at multiple time lags, and 3) investigate the changes in climate-carbon feedback at the regional scales.

## 2 Methods

### 2.1 Data

We used the Community Earth System Model (version 2) (CESM2) simulations at 1° × 1° spatial and monthly temporal resolution to analyze the climate driven extreme events in the net biome production. The CESM2 is a fully coupled global  
85 climate model comprising of land, atmosphere, and ocean components. The simulations analyzed here were forced with historical (1850–2014) and shared socioeconomic pathway 8.5 (SSP585; 2015–2100) scenarios, wherein atmospheric CO<sub>2</sub> rises from 280 ppm in 1850 to 1150 ppm in 2100 (Danabasoglu et al., 2020). While CO<sub>2</sub> forcing causes temperature to increase and

land-use changes have a slight cooling effect (Lawrence et al., 2019), resulting in an overall increase of about 8°C mean air temperature over the global land surface during 1850–2100.

## 90 2.2 Definition and Calculation of Extreme Events

The Intergovernmental Panel on Climate Change (IPCC) (Seneviratne et al., 2012) defines extremes of a variable as the subset of values in the tails of the probability distribution function (PDF) of anomalies. Based on the global PDF of NBP anomalies, we selected a threshold value of  $q = 5$ , such that total positive and negative extremes comprise of 5% of all NBP anomalies (schematic Figure S1). The negative and positive extremes in NBP extremes comprised of NBP anomalies smaller than  $-q$  and 95 larger than  $q$ , respectively. For any period, while the total number NBP extremes were constant (i.e. 5% of all NBP anomalies), the count and intensity among positive and negative extremes vary depending on nature of the PDF of NBP anomalies.

We computed extremes for every 25 year period from 1850 through 2100 to analyze the changing characteristics of NBP extremes at regional to global scales. For regional analysis, we used the 26 regions defined in the IPCC Special Report on Managing the Risks of Extreme Events and Disasters to Advance Climate Change Adaptation (Seneviratne et al., 2012), 100 hereafter referred to as the SREX regions (Figure S2). We analyzed the characteristics of NBP extremes during carbon uptake period when photosynthesis dominates NBP and land is a net sink of carbon ( $NBP > 0$ ) and carbon release period when NBP is dominated by respiration and disturbance processes and land is a net source of carbon ( $NBP < 0$ ) (Marcolla et al., 2020).

The anomalies in NBP were calculated by removing the modulated annual cycle and non linear trend from the time series of NBP at every grid cell. We calculated the modulated annual cycle and non linear trend of NBP using singular spectrum analysis 105 which is a non-parametric spectral estimation method that decomposes a time series into independent and interpretable components of predefined periodicities (Golyandina et al., 2001). The conventional way of computing annual cycle or climatology does not capture the intrinsic non-linearity of the climate-carbon feedback (Wu et al., 2008). The modulated annual cycle, comprised of signals with return period of 12 months and its harmonics, is able to capture varying modulation of seasonality 110 of NBP under rising CO<sub>2</sub> emissions. The non non linear trend comprised of the return periods of 10 years and higher such that the anomalies in the ecosystem and climate drivers capture the effects of the ENSO, which is believed to have a large impact on climate and carbon cycle (Zscheischler et al., 2014; Ault, 2020). Thus, NBP anomalies consists intraannual variability represented by high-frequency signals (<12 months) and the interannual variability (>12 months and <10 years).

## 2.3 Attribution to Climate Drivers

While most studies traditionally attribute the impact of changes in climate on carbon cycle at seasonal to annual time scales, 115 many responses and variability of climate and its impact on carbon cycle happen at shorter daily to monthly time scales (Frank et al., 2015). Some recent studies have performed attribution by comparing the median of the climate driver distribution in a large space-time dimension (Zscheischler et al., 2014; Flach et al., 2020), which may not capture the variability at regional to the grid cell scales. Using linear regression of time-continuous NBP extremes that represent the large intra- and inter-annual variation in NBP with climate anomalies, we quantified the dominance (regression coefficient) and response (sign of regression 120 coefficient) of climate drivers on large NBP extremes. The NBP extreme events could either occur contiguously over time and

space or isolated from other events. The long duration time-continuous extreme events have a larger impact on the terrestrial ecosystem than time-separated isolated extreme events. Similar to Sharma et al. (2022), we define time-continuous extreme (TCE) events that fulfill the following conditions, (i) it must consist of isolated extremes that are continuous for at least one season length (i.e., 3 months) and (ii) any number of isolated or contiguous extremes can be a part of a TCE event if the gap among such extremes is less than season length (i.e. up to 2 months). We assume that gaps greater than or equal to one season length as a separate TCE event.

Human activities such as fossil fuel emissions and land use changes modify biogeochemical and biogeophysical processes which alter the climate and climate-carbon feedbacks. Large anomalous changes in climate drivers have a strong impact on carbon uptake and biome productivity. Here, we attributed NBP TCEs to climate drivers, namely, precipitation (“Prcp”), soil moisture (“SM”), monthly average daily temperature (“TAS”), and carbon mass flux into atmosphere due to CO<sub>2</sub> emission from fire (“Fire”). As the terrestrial vegetation has ingrained plasticity to buffer and push back effects of climate change (Zhang et al., 2014), the impact of change in climate driver is often associated with lagged response. Moreover, the strength of the impact of climate on NBP is dependent on location, timing, and land cover type (Frank et al., 2015). The linear regression of TCEs in NBP and anomalies of every climate driver was performed at all qualifying land grid cells for lags from one to four months. We assumed that the higher the Pearson Correlation coefficient ( $\rho$ ) of a climate driver with NBP extremes, the larger is its impact on NBP at that location. The attribution based on  $\rho$  is used only for those grid cells where the significance value ( $p$ ) < 0.05. The grid cells with at least two negative and positive NBP TCEs each often yielded high correlation coefficients with high significance value ( $p$  < 0.05), thus this constraint was applied for attribution to climate drivers.

The instantaneous impact (when lag equals zero) of driver anomalies ( $dri_t$ ) on NBP TCEs ( $nbp_t$ ) is computed using the Equation 1, where  $N$  represents the months in TCEs at any grid cell. Attribution based on the lagged response of anomalous driver anomalies on NBP TCEs is computed using Equation 2, where  $L$  represents the number of lagged months. For lags greater than one month, we compute the correlation of the average of climate drivers anomalies,  $\frac{dri_{t-l}}{L}$  for every time-step in the driver anomalies, with  $nbp_t$ . The resulting  $\rho$  captures the average response of antecedent climatic conditions up to  $L$  months that drive NBP TCEs.

145

for lag = 0:

$$\rho = \text{corr}(dri_t, nbp_t) \mid t \in N \quad (1)$$

for lag >0:

$$\rho = \text{corr}\left(\sum_{l=1}^{l=L} \left(\frac{dri_{t-l}}{L}\right), nbp_t\right) \mid t \in N \quad (2)$$

The direction and strength of the impact of various climate drivers on plant productivity and carbon sink vary with space and time. The increased temperature could lead to increased respiration and losses in NBP in tropics and mid-latitudes, but an

155 increase in temperature could lead to higher photosynthetic activity in higher latitudes. A moderate reduction in precipitation may not severely impact the vegetation productivity, but if accompanied by heatwave could lead to large losses in NBP. We analyzed dominant climate drivers across SREX regions for every 25 year period from 1850 to 2100 to understand the changing characteristics of large spatio-temporal extremes and its drivers across time and space.

160 The anomalous climate drivers causing NBP extremes may or may not qualify as climate extremes by themselves. A recent study has found that the extreme years of climate and NBP are often not the same, and the compound effect of non-extreme climate drivers could drive an extreme in NBP (Pan et al., 2019). Since the occurrence of a NBP extreme is likely driven by compound effect of multiple climate divers, we identified co-occurring anomalous climatic conditions during and antecedent to NBP extremes to improve our understanding of the interactive compound effect of drivers on carbon cycle. The dominance of climate drivers are usually quantified by correlation coefficient's range of 0.5 – 0.7 (Dormann et al., 2013), we imposed a 165 limit of correlation coefficients  $> 0.6$  and significance values  $< 0.05$  on co-occurring individual climate drivers to qualify as individual or compound drivers of NBP extremes. These constraints yield a few number of extremes attributable to climate drivers with high confidence.

### 3 Results and Discussion

#### 3.1 Characteristics of NBP Extremes

170 The 5<sup>th</sup> percentile NBP anomalies computed every 25 year period from 1850 to 2100 render threshold trajectories increasing from 140 GgC/month to 220 GgC/month (Figure 1(a)). This 1.5 times increase in threshold values demonstrates the increasing magnitude of anomalies and interannual variability of NBP across the globe. Corresponding time series of intensity of losses and gains in biome productivity were calculated by integrating the negative (NBP anomalies  $< -q$ ) and positive (NBP anomalies  $> q$ ) extremes anomalies. The rate of increase in the magnitude of negative extremes ( $-834 \text{ MgC/month}$ ) was larger than 175 the positive extremes ( $804 \text{ MgC/month}$ ) (Figure 1(b)) which implies that over time the net losses in carbon storage during NBP extremes increases.

180 The changes in NBP are driven by spatial and temporal variations in climate drivers and anthropogenic forcing. During 1850–1874, 24 out of 26 regions were dominated by carbon release period and the total NBP was less than zero (Figure S3). From 1850 through 1960s, there was a net CO<sub>2</sub> influx into the atmosphere likely driven by deforestation, fire and land-use change activities (Friedlingstein et al., 2019) (Figure S9). After the year 1960, the reduction in the rate of deforestation and increase in fossil fuel emission raised the atmospheric CO<sub>2</sub> concentration. Increasing CO<sub>2</sub> fertilization, water-use efficiency, and lengthening of growing seasons enhanced vegetation growth and NBP with a large increase in tropics and northern high latitudes (Figure S4). After 2070, the total NBP reaches its peaks and starts to decline (Figure S3) as the ecosystem respiration exceeds total photosynthetic activity. The tropical region have the largest magnitude of NBP however the rate of increase of 185 NBP reduces after 2050 and the region of Sahara (SAH) shows an early decline in total NBP after the year 2050. Longer dry spells and intense rains due to changing precipitation patterns in the Mediterranean and subtropical ecosystems are likely to cause higher tree mortality (Frank et al., 2015). Hot temperatures and reduced activity of RuBisCO hindering carboxylation

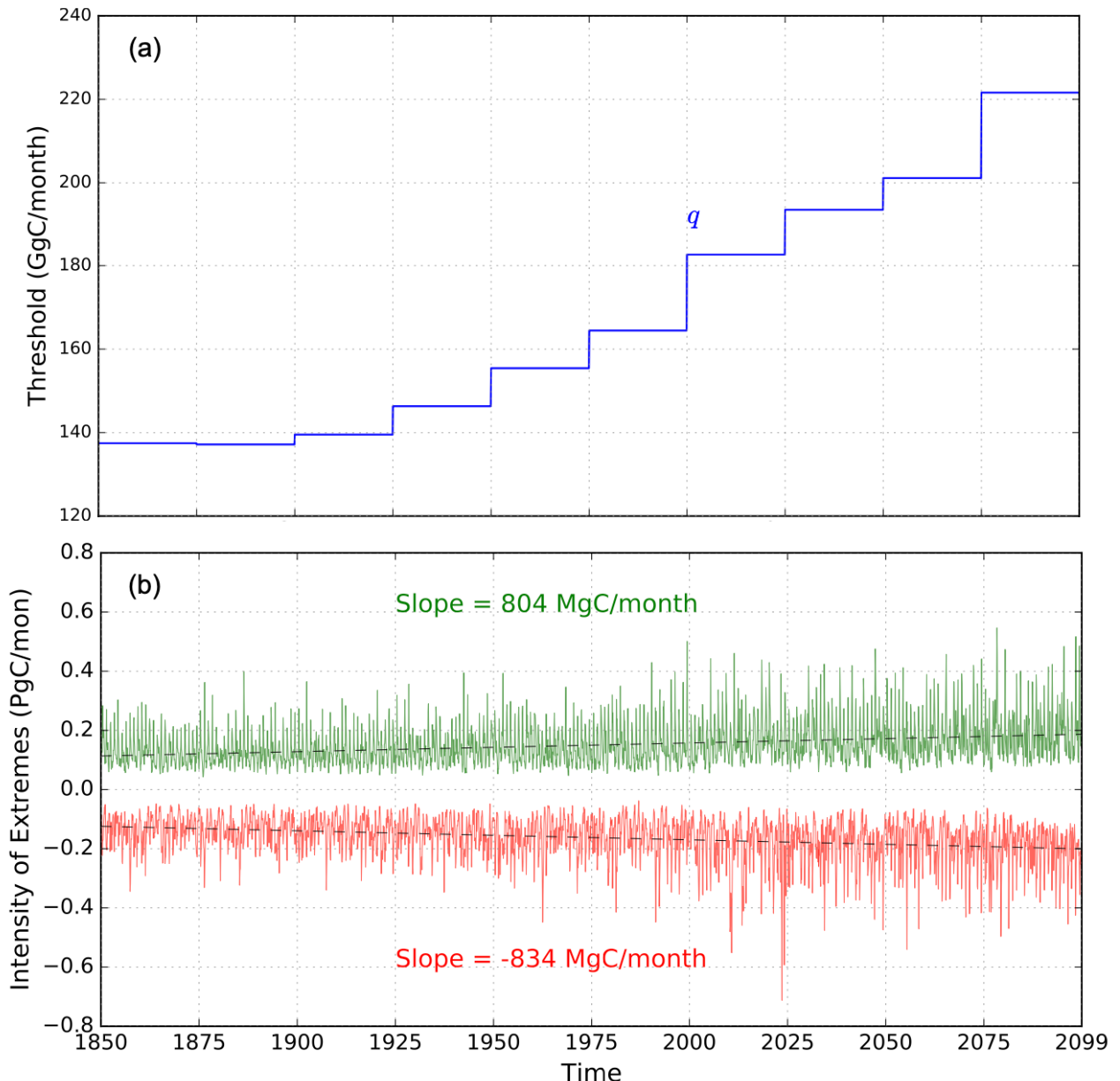


**Figure 1.** (a) The 5<sup>th</sup> percentile threshold,  $q$ , of NBP anomalies. The negative extremes in NBP are those NBP anomalies that are  $< -q$  and positive extremes are  $> q$ . (b) The intensity of positive and negative extremes in NBP in CESM2 are represent by green and red color, respectively. The rate of increase of positive and negative extremes in NBP are 804 and  $-834$  MgC per month.

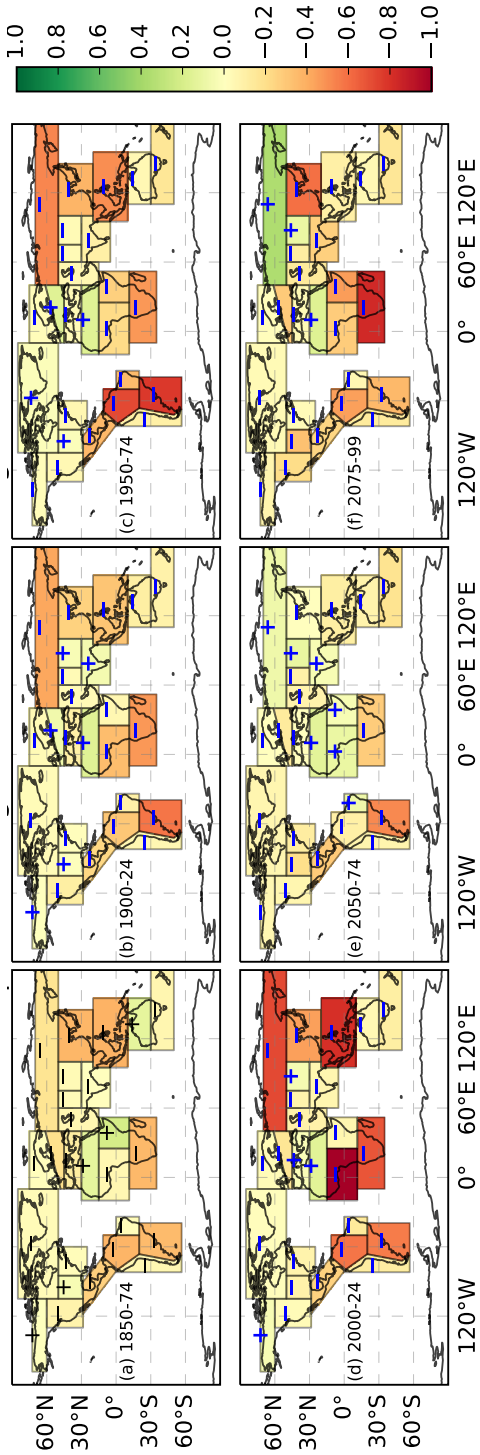


**Figure 2.** The sum of positive and negative carbon cycle extremes is referred as Net Uptake Change during NBP extremes. The figure shows the changing spatial distribution of net uptake change ( $\text{PgC}$ ) during following periods: (a) 1850–74, (b) 1900–24, (c) 1950–74, (d) 2000–24, (e) 2050–74, and (f) 2075–99. Net gain in carbon uptake is represented by green color and '+' sign; net decrease is represented by red color and '-' sign. At most regions, the magnitude of negative NBP extremes or losses in carbon uptake are higher than positive NBP extremes or gains in carbon uptake.

are the possible factors that will cause a net decrease in NBP in the region of SAH and make it a net carbon source after 2050.

During 2050–74 and 2075–99, the low-latitude regions exhibit the highest regional NBP; however, many regions in the tropics

190 witness a declining growth rate of regional NBP (Figure S4).

As anomalous changes in climate vary over space and time, the extremes in NBP also respond to the interactive effects of climate drivers and exhibit spatial and temporal variation. Figure 2 shows net total sum of both positive and negative extremes in NBP in SREX regions integrated for 25 year periods (1850–74, 1900–24, 1950–74, 2000–24, 2050–74, and 2075–99). Most regions exhibit net losses in the biome productivity during extremes, e.g. South Africa (SAF) has always been dominated by negative NBP extremes. The large magnitude of net carbon uptake changes during the period 2000–24 was likely driven by a change in LULCC forcing from decadal to annual during 2000–2015 and then back to decadal 2015 onward. The change in resolution of LULCC forcing possibly caused higher climate variability due to biogeophysical feedbacks and subsequently led to increased carbon cycle variability and extremes. 23 out of 26 SREX regions experience an overall loss in biomass productivity during extremes during the end of the 21<sup>st</sup> century (Figure 2). The distribution of the total magnitude and count of negative TCEs during 2075–99 across all the SREX regions follow a similar pattern i.e., more frequent the extremes larger were the carbon losses (Figure 3(a)). The largest losses in carbon uptake during TCEs were in tropical regions, e.g., East Asia (EAS), Amazon (AMZ), and SAF, with –3, –3, and –2.25 PgC carbon loss during 2075–99. These regions also witness the highest number (1270, 1410, 950) of negative NBP TCEs. The magnitude of carbon losses and the number of negative NBP TCEs were highest in tropical regions. The magnitude and number of negative TCEs were very low for high latitude of Alaska (ALA), Canada and Greenland (CGI), Eastern North America (ENA), North Europe (NEU), Central Europe (CEU), and dry regions of Mediterranean (MED) and Sahara (SAH). Although the number of NBP TCEs in NAS are more than Southeastern South America (SSA) and Central America (CAM), the magnitude of NBP TCEs in NAS are low due to less regional NBP. Since the extremes were calculated based on global anomalies, the largest impact on terrestrial carbon uptake are expected in the regions of AMZ, EAS, and SAF.

210 The magnitude and the total number of regions dominated by negative extremes in NBP are expected to gradually increase in the 21<sup>st</sup> century (Figure 3(b)). Most of the increase in the frequency of negative extremes in NBP are expected in ENA, South Asia (SAS), SAF, and CAM (Figure S5). The increase in the magnitude (23 out of 26 or 88% of regions) and frequency (18 out of 26 or 70% of regions) of negative NBP TCEs in most SREX regions during 2075–99 is a matter of concern since the total global NBP peaked at around 2070 and declines further in the model (Figure S3). The negative NBP TCEs dominate in

215 eight out of nine tropical regions, which store the largest standing carbon biomass and represent the largest portion of carbon uptake loss during negative NBP extremes. A large magnitude of extreme events in the NBP could potentially lead to a state of low and decreasing carbon sink capacity which further lead to positive feedback on climate warming. The strengthening of negative extremes relative to positive extremes in NBP is of concern to future terrestrial carbon sink capacity (Figure S3).

The positive feedback of warming and climate driver losses in carbon uptake posses many concerns about the implications 220 of reducing terrestrial uptake capacity on food security, global warming, and ecosystem functioning. Moreover, the biological system's sensitivity is higher for climate and carbon extremes than for gradual changes because of larger response strength and shorter response times (Frank et al., 2015).

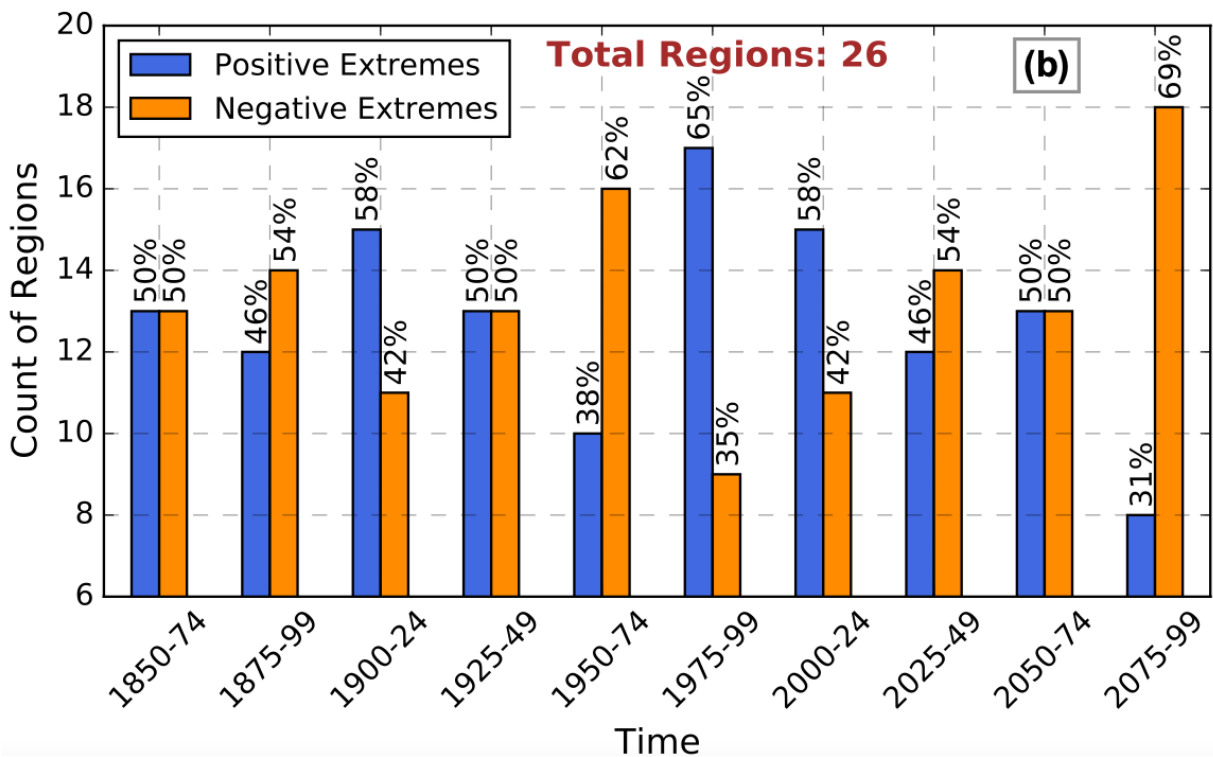
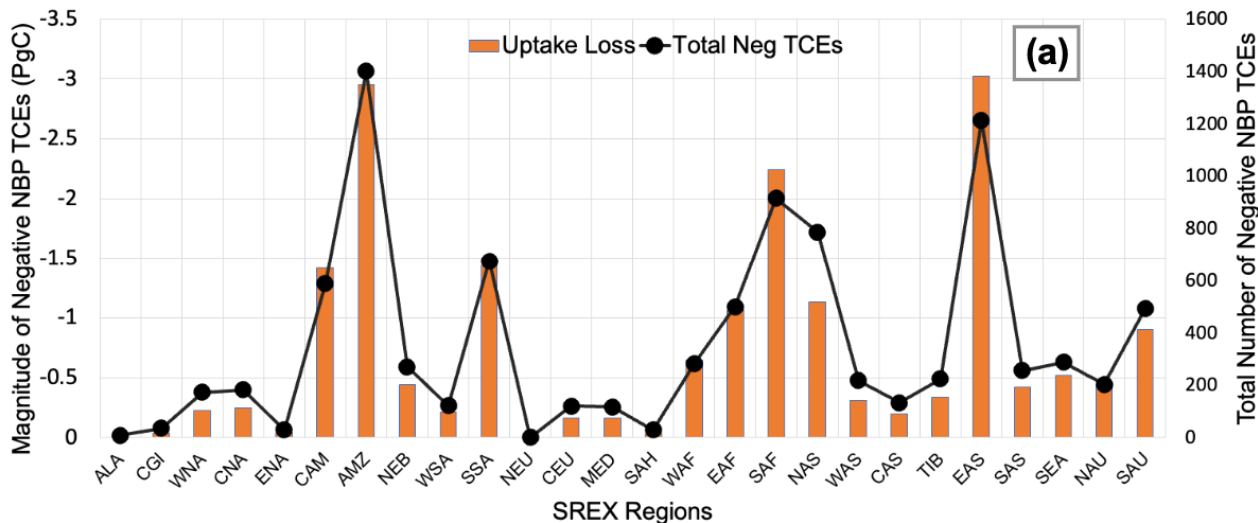


**Figure 3.** (a) Total magnitude of negative carbon cycle extremes or loss is carbon uptake during TCEs across SREX regions plotted as bar graph (left y-axis). Total number of negative TCE events (right y-axis) plotted as line graph. The largest portion of carbon uptake loss is in tropical SREX regions of Amazon (AMZ), East Asia (EAS), and South Africa (SAF) for the period 2075-99. (b) Count (y-axis) of the regions dominated by either positive or negative NBP extremes. Relative to a total of 26 SREX-regions, the percent count of positive or negative NBP extremes is represented at the top of the bars.

### 3.2 Attribution to Climate Drivers

The increase in climate variability and extremes driven by rising CO<sub>2</sub> emissions influences the terrestrial carbon cycle (von 225 Buttlar et al., 2018; Reichstein et al., 2013; Sharma et al., 2022). The influence of climate drivers on NBP extremes is dependent on the regional interannual variability of climatic conditions and vegetation composition. The percent of total number of grid cells which show soil moisture as a dominant driver of NBP TCEs were about 40 to 50 percent from 1850 to 2100 across multiple lags, which means that the near term and long term impact of soil moisture were highest among other drivers (Figure S6). The positive response of soil moisture anomalies on NBP TCEs indicate that a decline in soil moisture causes a 230 reduction in NBP and vice-versa. Likewise, the dominant climate driver across 26 SREX regions was also soil moisture and with positive response relationship with NBP TCEs (Figure 4). However, the percent of total number of grid cells dominated by precipitation doubled (10 to 20 percent) when lag was increased from 1 to 3 months. This implies that antecedent declines in precipitation limits carbon uptake more than recent decline in precipitation and possibly causes a decline in soil moisture. Moreover, the plants with deep roots are less impacted with short-term reduction in precipitation than prolonged droughts 235 which are caused by soil moisture limitation. By the end of the 21<sup>st</sup> century, the model suggest that 70% of the total number of NBP extremes will be water-driven i.e. due to soil moisture and precipitation. Our results were consistent with the recent studies (Liu et al., 2020; Pan et al., 2019) that have found that the most important factor limiting vegetation growth is dryness stress which is caused mainly by low soil moisture and lack of soil moisture for longer periods could result in drought events, causing a larger reduction of ecosystem productivity and smaller reduction of terrestrial respiration.

240 The second most dominant driver of NBP TCEs was fire which has a positive response on NBP TCEs (Figure S6). Fire is an important Earth system process that is dependent on vegetation, climate, and anthropogenic activities. CESM2 incorporated a process-based fire model, which contains three components, namely, fire occurrence, fire spread, and fire impact (Li et al., 2013). The interannual variability of agricultural fires is largely dependent on fuel load and harvesting; deforestation fires included fires due to natural and anthropogenic ignitions, caused by deforestation, land-use change, and dry climate. Peat fires 245 usually occur in the late dry season and are strongly controlled by climate. The current version of the fire model reasonably simulates burned area, fire seasonality, fire interannual variability, and fire emissions (Li et al., 2013). As fires are controlled by soil moisture, temperature, and wind, the attribution of NBP extremes to fires could also include the NBP extremes that could be driven by lack of soil moisture and hot temperatures. Therefore, total number of fires events could be larger and recovery after such fire driven extremes could be much longer.

250 Hot temperatures if persists for long periods causes heatwaves which tend to reduce ecosystem production and enhanced terrestrial respiration causing a large reduction in NBP (Pan et al., 2019). The leaf photosynthesis depends on RuBisCO limited rate of carboxylation which is inversely proportional to the Q<sub>10</sub> function of temperature (Lawrence et al., 2019). Hubau et al. (2020) found that with increasing temperatures and droughts, the tree growth has been reduced and could offset the earlier gains. On the contrary, warm temperatures in the northern high latitudes cause an increase in carbon uptake due to reduced snow cover 255 and optimal temperature for photosynthesis. Increased warming at northern high latitudes could lead to hot temperature-related hazards and alter temperature-carbon interactions, details discussed in Section 3.5.

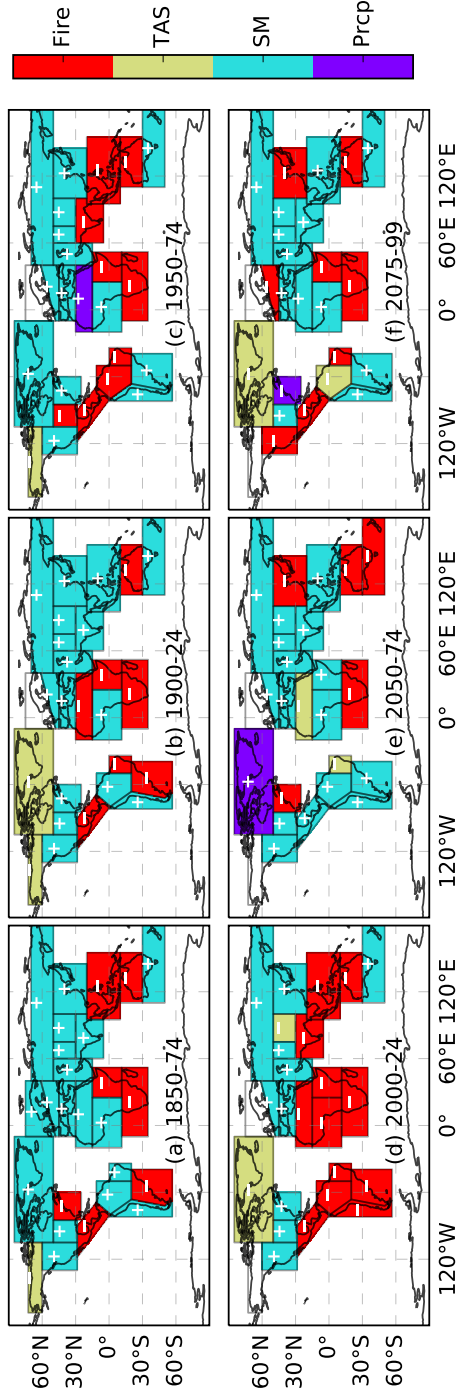


**Figure 4.** Spatial distribution of dominant climate drivers across SREX regions. The color in every SREX region represents the most climate driver causing carbon cycle extremes at 1 month lag for following periods: (a) 1850–74, (b) 1900–24, (c) 1950–74, (d) 2000–24, (e) 2050–74, and (f) 2075–99. The positive ('+') and negative ('−') sign within a region represents the correlation relationship of NBP extremes with every dominant climate drivers.

Rising CO<sub>2</sub> emissions drive high temperature in tropics and have the potential to hinder photosynthesis and vegetation growth, further discussed in Section 3.4. The changes in atmospheric circulation patterns might also influence the precipitation cycle resulting in longer dry spells and could increase fire risks with canopy closure (Frank et al., 2015; Langenbrunner et al., 260 2019). The second-largest magnitudes of negative NBP extremes are witnessed by arid and semi-arid regions with mostly grasslands (Figure 3(a)). Several studies conclude that soil moisture causes an increase in dry days and a significant negative effect on the carbon cycle driven by increasing droughts in arid, semi-arid, and dry temperate regions (Frank et al., 2015; Zscheischler et al., 2014; Pan et al., 2019). The regions of South Africa, Central America, and Northern Australia witness the largest NBP extremes driven by fire. The region of Amazon was dominated by fire, soil moisture, and temperature in the 21<sup>st</sup> 265 century. Reduction of fuel load by changing vegetation (PFT) composition could likely be the reason for lesser fire-dominated regions later in the 21<sup>st</sup> century.

### 3.3 Compound Effect of Climate Drivers

The interactive effect of multiple climate drivers could lead to devastating ecological consequences as compound extremes often have a larger impact on the carbon cycle than the aggregate response of individual climate drivers (Zscheischler et al., 270 2018; Ribeiro et al., 2020; Pan et al., 2019). We used three broad classes of climate drivers, namely, moisture (dry vs wet), temperature (hot vs cold), and fire to study their compound effect. At most grid cells, NBP extremes were either positively correlated with anomalous precipitation and (or) soil moisture, and (or) negatively correlated with temperature and (or) fire. Figure 5 shows the compound climate drivers, both mutually exclusive and inclusive, driving NBP extremes over time. Mutually 275 exclusive drivers are those climatic conditions that do not occur at the same time to cause an extreme event. When the drivers of an extreme are overlapping they are called mutually inclusive. For example, if an extreme is driven by both *hot* and *dry* conditions, the mutually exclusive climate driver is only *hot & dry* and the mutually inclusive drivers are *hot, dry*, and *hot & dry*.

The largest fraction, about 50%, of total NBP TCEs were attributed to the combined effect of *hot & dry & fire* events (Figure 5). This implies that every other large extreme event associated with anomalous loss in biome productivity was driven 280 by the interactive effect of water limitation, hot days (heat waves) and both of which together could trigger fire and loss of carbon. The second strongest exclusive compound driver was *dry & fire* causing about 25% of extremes. With increasing climate warming, the number of NBP extremes driven by hot and dry climatic conditions have increased, with about 10% extremes driven exclusively by *hot & dry* events during 2050–74.

Although the negative impact of water limitation (*dry*) on NBP extremes was the highest (driving inclusively about 90% of 285 all NBP extremes), rising emissions and climate change will lead to increasing number, 54% during 1900–24 to 62% during 2050–74, of NBP extremes driven inclusively by *hot* climatic conditions (Figure 5). For the same periods, an 8% increase in extremes driven inclusively by *hot & dry* is expected.

The effect of rising temperature on vegetation growth and carbon uptake is dependent on the geographical location. Pan et al. (2019) found that net ecosystem production had a negative sensitivity to warming across 81 percent of the global vegetated land area during 2007–18 and only the higher latitudes and Tibetan Plateau (TIB) had a positive sensitivity of NBP 290

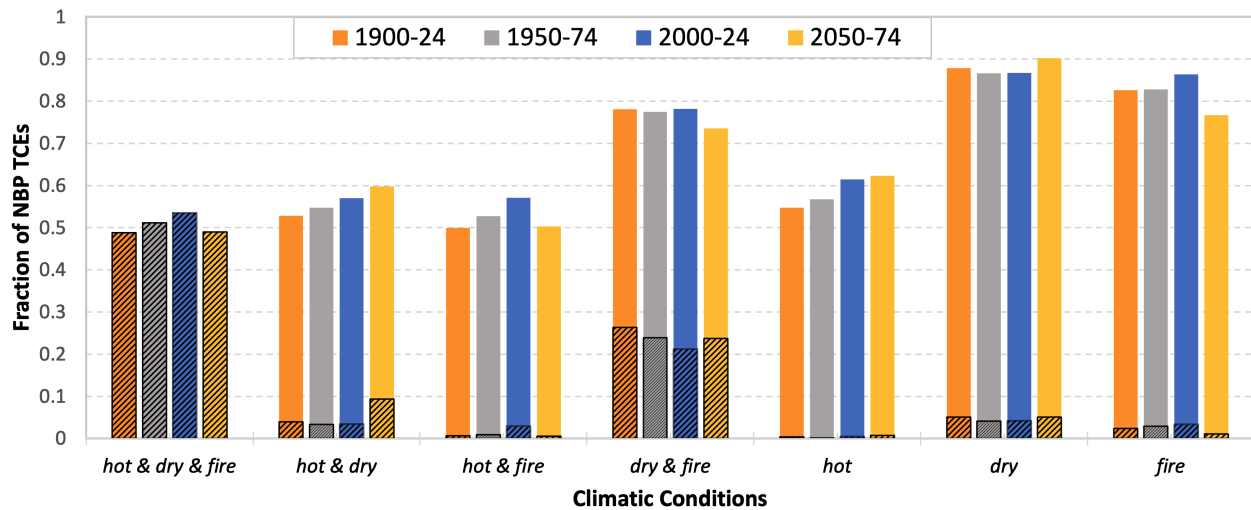


**Figure 5.** Fractional distribution of carbon cycle time-continuous extremes (TCEs) driven by compound climate drivers at lag of 1 month. The unhatched and hatched bars represent the mutually inclusive and exclusive compound and individual climate drivers, respectively. The exclusive climate drivers are always less than or equal to mutually inclusive drivers. The different colored bar represents following periods: 1900–24, 1950–74, 2000–24, and 2050–74 (from left to right bar). Most carbon cycle extremes are driven by interactive effect of climate drivers.

to temperature. Similarly, Marcolla et al. (2020) found a positive sensitivity of NBP to air temperature in higher latitudes and negative sensitivity in tropics. As tropics have the largest standing biomass and high latitude regions have largest stored carbon, understanding the impact of climate change across these regions is important. The next two sections will briefly discuss the changing characteristics of extremes in tropics and high latitudes.

#### 295 3.4 Increasing temperature sensitivity and weakening terrestrial carbon sink across Tropics

Observation based studies have reported a decline in the rate of carbon uptake in Amazonian forest, and expect similar decline in African tropics in future (Hubau et al., 2020). Over long timescales, the rising atmospheric CO<sub>2</sub> concentration may not necessarily leads to an increase plant biomass (Walker et al., 2019) as respiration losses outpace the net uptake. Increasingly frequent and stronger heatwaves, droughts, and fires due to climate change are likely to cause the growth rate of NBP to flatten 300 out by late 21<sup>st</sup> century (Figure S9). They may lead to an eventual reduction in total stored carbon and potential reversal of tropical vegetation from a net carbon sink to a carbon source. Towards end of 21<sup>st</sup> century (2075–99), most of the SREX regions (23 of 26) are dominated by negative NBP extremes (Figure 3(b)), especially in tropical region (CAM, AMZ, NEB, WAF, EAF, SAF, SAS, SEA, and NAU) (Figure 2). During 2075–99, almost all tropical SREX regions (with the exception of NAU) are dominated by negative NBP extremes.

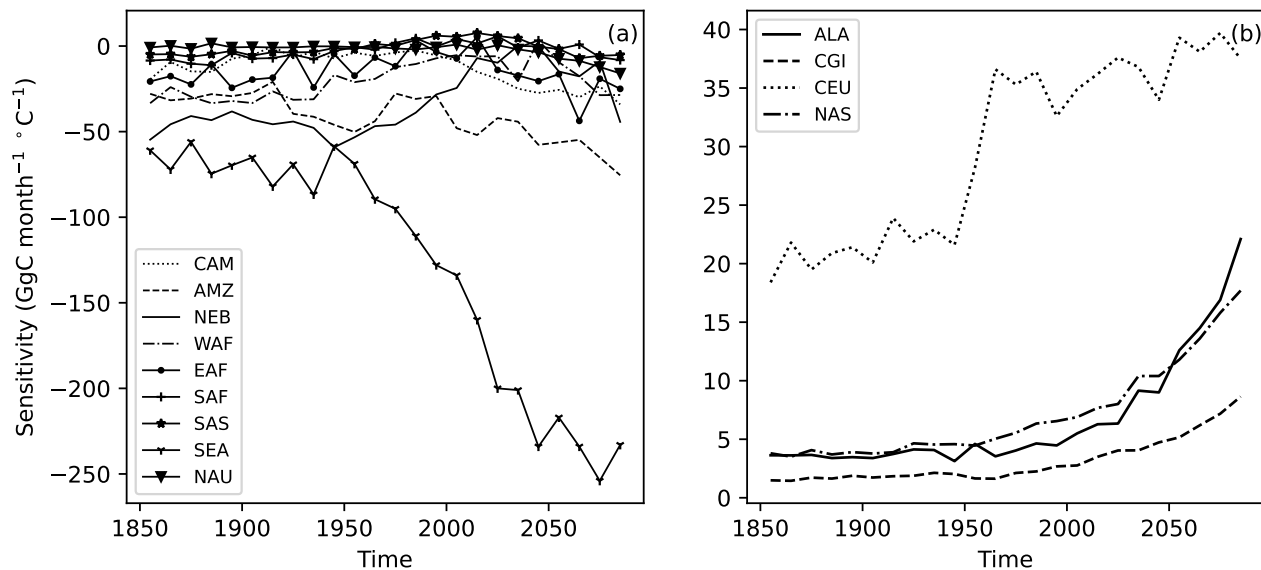


**Figure 6.** Changing temperature sensitivity of detrended anomalies in NBP to detrended anomalies in surface temperature for 10 year time periods at multiple SREX regions. The regions at low latitudes (a) have negative NBP sensitivity to temperature anomalies and high latitudes (b) have positive sensitivities.

305     Rising temperature and atmospheric CO<sub>2</sub> lead to increasing trend for GPP and NPP across most of the tropics. However, they are often also accompanied by increase in disturbances (such as droughts, and fire), inducing plant mortality and increase in heterotrophic respiration contributing to a significant quantities of negative carbon fluxes from the ecosystem. With the exception of AMZ and SEA that continue to see an increase in NBP in the model simulation, most of the tropical region show a 310 saturation or decline in NBP towards the end of 21<sup>st</sup> century (Figure S9). Analysis of temperature trends across tropical regions show a significant trend towards warmer temperatures during warm (increase in 90<sup>th</sup> quantile) as well as cool (increase in 10<sup>th</sup> quantile) months of the year (Figure S7). Rising daily temperatures hinder net carbon uptake by enhancing stomatal closure and ecosystem respiration (Figure S9). The strength of 10 years negative temperature sensitivity of NBP (see Section S01) 315 increase over time (Figure 6(a)), suggesting an accelerated reduction in NBP growth with rising temperatures. The negative sensitivity values gradually increase from -20 GgC/month·°C to -33 GgC/month·°C for CAM, and -30 GgC/month·°C to -70 GgC/month·°C for AMZ during 1850-2100. South-East Asia (SEA) saw the highest negative temperature sensitivity of -207 GgC/month·°C by the end of 21<sup>st</sup> century. Similar patterns are seen in other tropical regions suggesting an increasing negative temperature sensitivity of terrestrial ecosystem to uptake carbon in a warming world (Figure 6(a)).

### 3.5 High latitude ecosystem can potentially becomes source of carbon under warming climate

High latitude ecosystems store large amounts of carbon below ground and increasing exposure to warming and disturbance 320 pose the risk of release of stored soil carbon (Marcolla et al., 2020) into the atmosphere. Warmer temperatures at high lati-

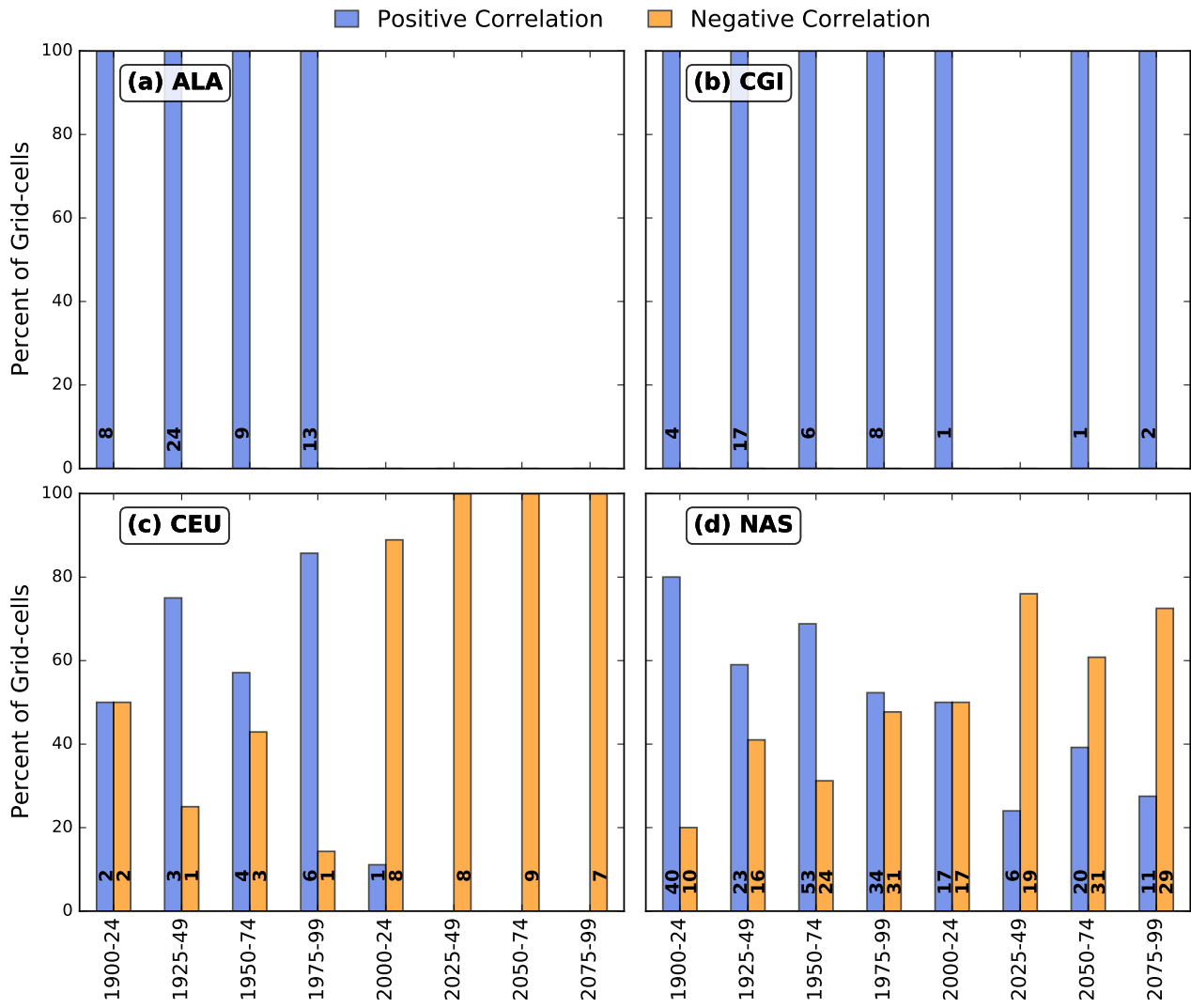


**Figure 7.** Percent distribution of grid cells with positive and negative correlation of extreme NBP anomalies with temperature (TAS) anomalies at a lag of 1 month in the regions of (a) Alaska, (b) Canada, Greenland, and Iceland, (c) Central Europe, and (d) Northern Asia (NAS). The blue and orange color bars highlight the positive and negative correlations. The total number of grid cells that experienced NBP extremes and dominated by positive and negative correlations are shown in black at the bottom of the respected bars.

tudes create favorable conditions for longer growing season, enhanced plant growth and overall increase in greening. All high latitude regions (ALA, CGI, CEU, NAS) show a trend of positive and increasing NBP sensitivity to change in air temperature (Section S01) over 1850–2100 (Figure 6).

325 While overall impact of warming on high latitude carbon update is expected to be positive, on monthly scale an increasing number of events when warming leads to a net loss of carbon uptake is observed (Figure 7). The negative response of NBP to warm air temperature anomalies were found to occur most frequently during the summer months of July and August. Simulations analyzed show a strong trend of warming during warm months. For example, the 90<sup>th</sup> quantile temperature increased from 13°C by 8°C to 21°C quantile in NAS while similar increases were observed for ALA, CGI and CEU (Figure S8(d)). With warming temperature trends these periods of carbon losses in response to temperature extremes have outsized impact on overall carbon budget of the high latitude ecosystem. Towards end of the 21<sup>st</sup> century, CGI and NAS show strong decline in NBP becoming a net source of carbon.

FORREST: Please read the above paragraph and see if we can drop Figure 7 (histogram of positive/negative correlation). It can either move to supplement or just simply dropped. If reviewer question was conclusions, we can bring it back.

335 The accelerated warming of winter temperatures have large consequences for respiration losses in the Arctic and Boreal regions (Natali et al., 2019; Jones et al., 1998; Commane et al., 2017). Natali et al. (2019) found that the total carbon loss during winter respiration in Artic was 60% larger than the summer carbon uptake during 2003–17, driven primarily by higher soil and air temperatures. Contrary to insitu observations which show significant CO<sub>2</sub> emissions at subzero temperatures, current generation of process based models shut off the respiration at subzero temperatures, thus underestimating the carbon losses during winters (Natali et al., 2019). Simulation analyzed show a 1.7 times higher increase in winter air temperature 340 (10<sup>th</sup> quantile) compared to summer air temperature (90<sup>th</sup> quantile) at high latitudes (Figure S8). For example, in NAS, the 10<sup>th</sup> quantile temperature increased from –25°C during 1900–24 by 14°C to –11°C during 2075–99. The 90<sup>th</sup> quantile temperature increased from 13°C by 8°C to 21°C quantile over the same time period (Figure S8(d)). This enhanced rate of warming, especially during winter, results in rising winter and total ecosystem (auto- and hetro- trophic) respirations, turning some regions to net source of carbon (Figure S10).

345 With the warming of warm and cold season temperatures there is a potential risk of losing a carbon sink and an accelerated release of stored carbon into the atmosphere. The increase in hetrotrophic respiration is likely due to increased thaw of permafrost (Turetsky et al., 2020), higher litter pool due to accelerated GPP, and longer warm season for higher microbial decomposition. As a result, the peak of NBP and NEP starts to sharply decline towards the end of 21st century. The regions of CGI is expected to become carbon source by 2100 and the NBP of the region of CEU is gradually decreasing since 1975. 350 The NAS region has also reported a reduction in total NBP during 2075–2099, breaking the consistent increasing trend since 1850. With accelerated rising winter temperature (Figure S8), declining NEP and NBP (Figure S10) and underestimation of respiration in the current process models, the losses in carbon uptake in the Arctic and high latitudes are expected to be higher in the future.

## 4 Conclusions

355 Can/Should we use the term WARM instead of HOT for compound drivers?

Increasing frequency of climate change driven extremes such as fire, drought, and heatwaves have the potential to cause large loss of carbon from the terrestrial biomass storage. The increasing frequency and magnitude of negative NBP extremes and saturation of NBP towards the end of the 21<sup>st</sup> century raise questions about the continued ability of terrestrial ecosystem to sequester carbon and ameliorate the impact of climate extremes and change. Under changing climate, parts of the globe  
360 are expected to experience enhanced vegetation growth and thus positive extremes in NBP, however, they are far outpaced by the frequency and intensity of negative extremes and associated loss in NBP. At global scale, reduction in deforestation and enhanced CO<sub>2</sub> fertilization led to an increase in NBP reaching its peak around 2070 followed by large decline towards the end of the 21<sup>st</sup> century. These losses in NBP were particularly large in carbon rich tropical region, followed by arid and semi-arid regions of the world. During 2075–99, 23 out of 26 SREX regions are dominated by negative NBP extreme events, especially  
365 the tropical regions. Increasing intensity and magnitude of negative extremes in NBP towards the end of the 21<sup>st</sup> century and beyond could lead to widespread decline in vegetation, loss of terrestrial carbon storage, and potentially turn terrestrial ecosystem in a net source of carbon.

Extremes in carbon cycle, driven by the extremes in the environmental conditions, impact vegetation health and productivity. We analyzed anomalies in three primary environmental drivers (*hot, dry and fire*) of NBP extremes. Anomalies in soil moisture,  
370 causing widespread droughts and water stress in vegetation, was identified as the most dominant driver of negative NBP extremes affecting almost half of the grid cells experiencing NBP extremes. Interactive and compounded impact of simultaneous anomalies in multiple drivers especially have large impacts on the vegetation productivity, beyond the individual impacts of the variables. Extreme temperature anomalies compounded with dry conditions impact vegetation productivity, more than the sum of individual temperature and moisture anomalies. They also increase the risk and occurrence of fires. Compound effect  
375 of all three climate drivers (*hot, dry and fire*) cause the largest fraction of NBP TCEs.

In the tropics the growth rate of NBP is decreasing, the magnitude of negative extremes in NBP and negative temperature sensitivity of NBP is strengthening over time. Large standing carbon stock (fuel load) with hot and dry climate (fire weather conditions) increases the fire risk and potential loss of carbon stock during negative NBP extremes. In the northern high latitudes, accelerated warming leads to permafrost thaw and release of belowground carbon, increasing the likelihood of reversal  
380 of the ecosystem to a net source of carbon over time.

This study analyzed climate-driven NBP extremes using the CESM2 model simulation from 1850 to 2100. The future work will use multi-model model analysis to evaluate the agreement among different earth system models of magnitude, frequency, and spatial distribution of NBP extremes and their attribution to the individual and compound climate drivers. The longer-term simulations are needed to analyze the climate-carbon feedback post-2100 when the difference between rate of CO<sub>2</sub> emissions  
385 and terrestrial carbon uptake is expected to increase.

*Code availability.* Data analysis was performed in Python, and the analysis codes will be publically available on GitHub at [https://github.com/sharma-bharat/Codes\\_NBP\\_Extremes](https://github.com/sharma-bharat/Codes_NBP_Extremes) upon acceptance of manuscript.

*Data availability.* The data used here are from the CMIP6 simulations performed by the various modelling groups and available from the CMIP6 archive maintained by from Earth System Grid Federation (ESGF) <https://esgf-node.llnl.gov/search/cmip6>.

390 At the CMIP6 archive site <https://esgf-node.llnl.gov/search/cmip6> searching for a given model, a given experiment, and a given variable name will yield the link to the dataset that can be downloaded.

## Appendix: Supplementary

### S01 Calculation of temperature sensitivity of NBP

The sensitivity of NBP flux to surface air temperature is calculated using linear regression method (Piao et al., 2013),

395  $NBP_{detrended} = b_0 + b_1 \cdot TAS_{detrended} + \epsilon$  (S01)

where  $NBP_{detrended}$  refers to the detrended monthly timeseries of NBP and TAS refers to the detrended monthly timeseries of surface air temperature. The regression coefficient  $b_1$  represent the apparent sensitivity of NBP to TAS;  $b_0$  is the fitted intercept;  $\epsilon$  is the residue error in the linear regression. The sensitivities of tropical and high latitudinal regions, as shown in Figure 6, has been calculated for consequentive 10 years periods starting from 1850 to 2100. The detrended timeseries of NBP and TAS 400 for every SREX region were calculated by calculating the difference of area weighted mean and 10 year moving average of respective variables. Positive temperature sensitivity to NBP signifies strengthening the impact of temperature on net biome carbon flux and vice versa.

**Table S1.** SREX Reference Regions

Abreviation	Region's Full Name
ALA	Alaska/N.W. Canada
AMZ	Amazon
CAM	Central America/Mexico
CAS	Central Asia
CEU	Central Europe
CGI	Canada/Greenland/Iceland
CNA	Central North America
EAF	East Africa
EAS	East Asia
ENA	East North America
MED	South Europe/Mediterranean
NAS	North Asia
NAU	North Australia
NEB	North-East Brazil
NEU	North Europe
SAF	Southern Africa
SAH	Sahara
SAS	South Asia
SAU	South Australia/New Zealand
SEA	Southeast Asia
SSA	Southeastern South America
TIB	Tibetan Plateau
WAF	West Africa
WAS	West Asia
WNA	West North America
WSA	West Coast South America

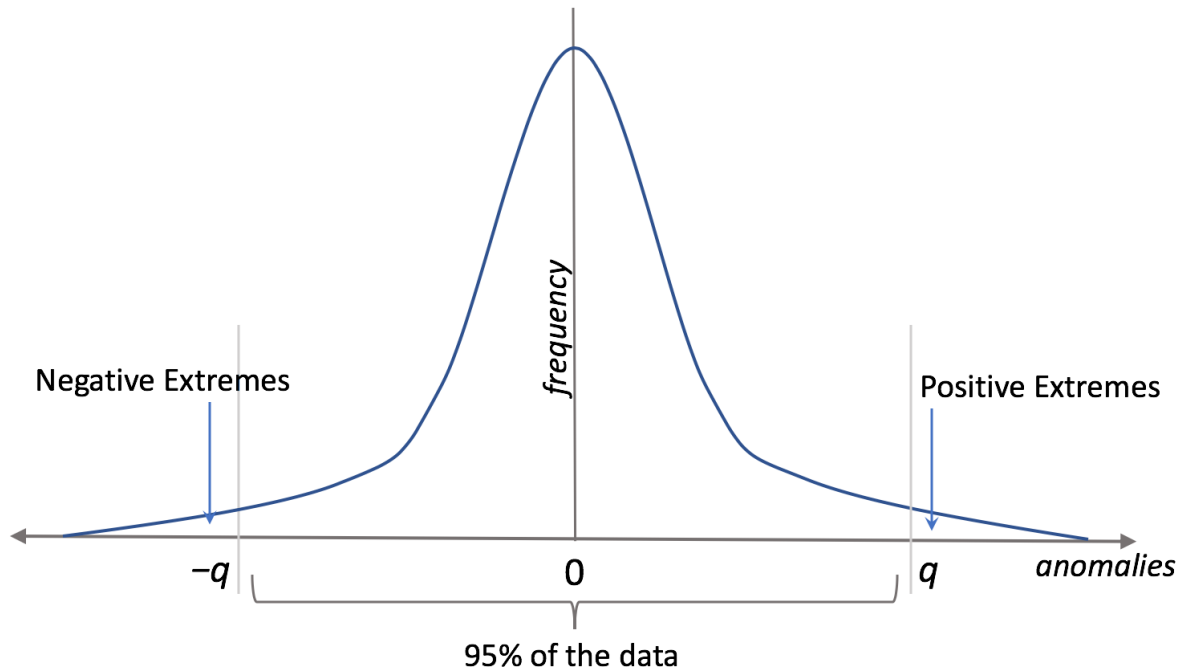


**Figure S1.** The schematic diagram representing the NBP extremes. The threshold  $q$  is set at  $5^{th}$  percentile in this study, such that 95% of the NBP anomalies lie within  $-q$  and  $q$ .

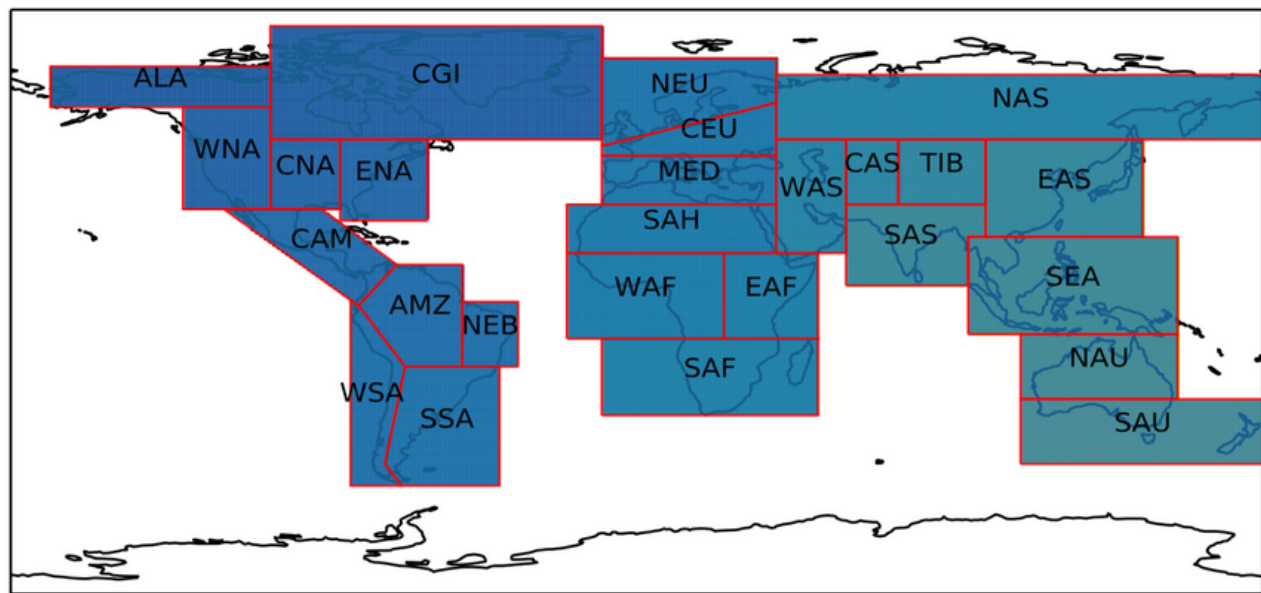


**Figure S2.** The spatial extent of SREX reference regions; abbreviations mentioned in the Table S1.

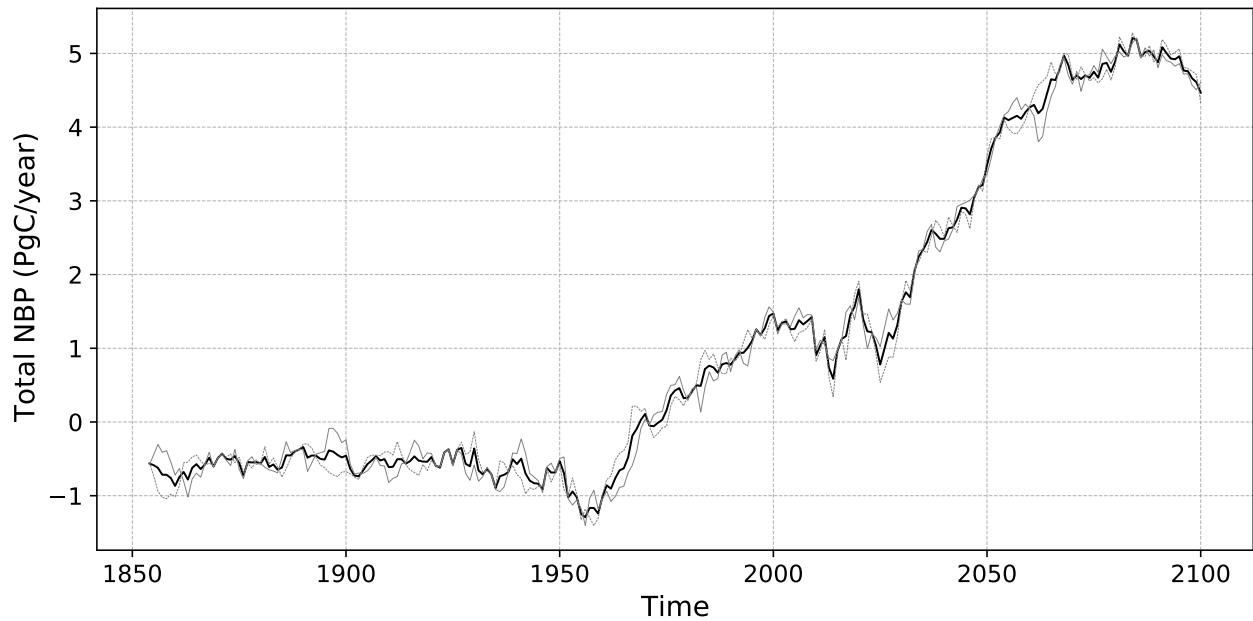


**Figure S3.** The timeseries of globally integrated 5 year rolling mean of NBP from 1850–2100 for CESM2 ensemble members is shown in gray dashed lines. The timeseries of globally integrated 5 year rolling mean of multi-ensemble mean is shown in black solid line.

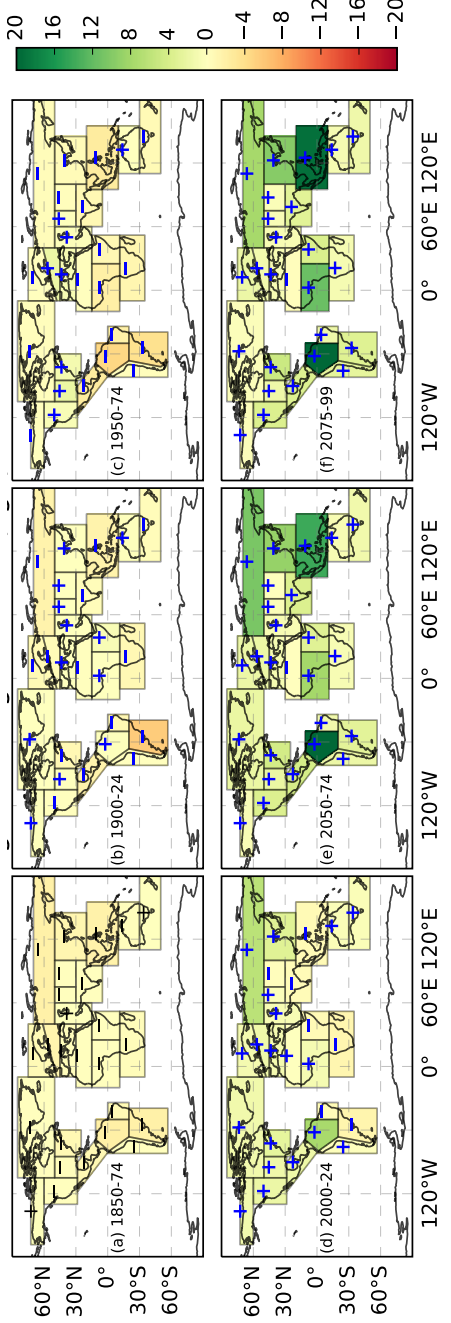


**Figure S4.** Total integrated NBP (PgC) for 25 years time windows of period 1850–2100. Spatial distribution of integrated NBP (PgC) change over time: (a) 1850–74, (b) 1900–24, (c) 1950–74, (d) 2000–24, (e) 2050–74, and (f) 2075–99. Net increase in regional NBP or total carbon uptake is represented by green color and ‘+’ sign; net decrease is represented by red color and ‘-’ sign.

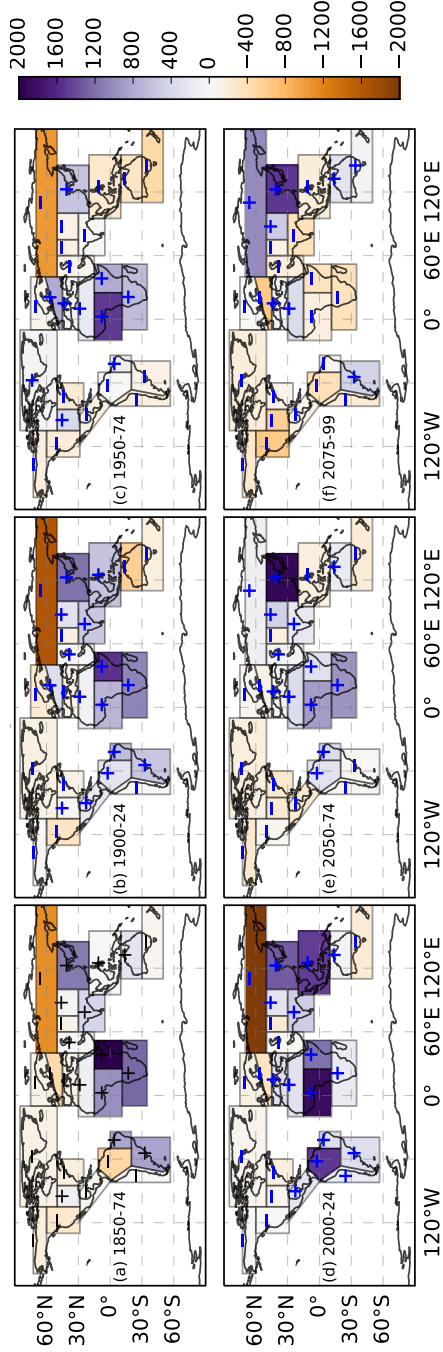


**Figure S5.** Frequency of positive *vs* negative NBP extreme events across SREX regions. Purple color ('+' sign) highlights the regions where frequency of positive NBP extremes events exceed negative NBP extremes; and brown color ('-' sign) identifies regions where frequency of negative NBP extreme events exceed positive NBP extremes. Towards the end of 21st century, most tropical regions are dominated by frequent negative NBP extremes.

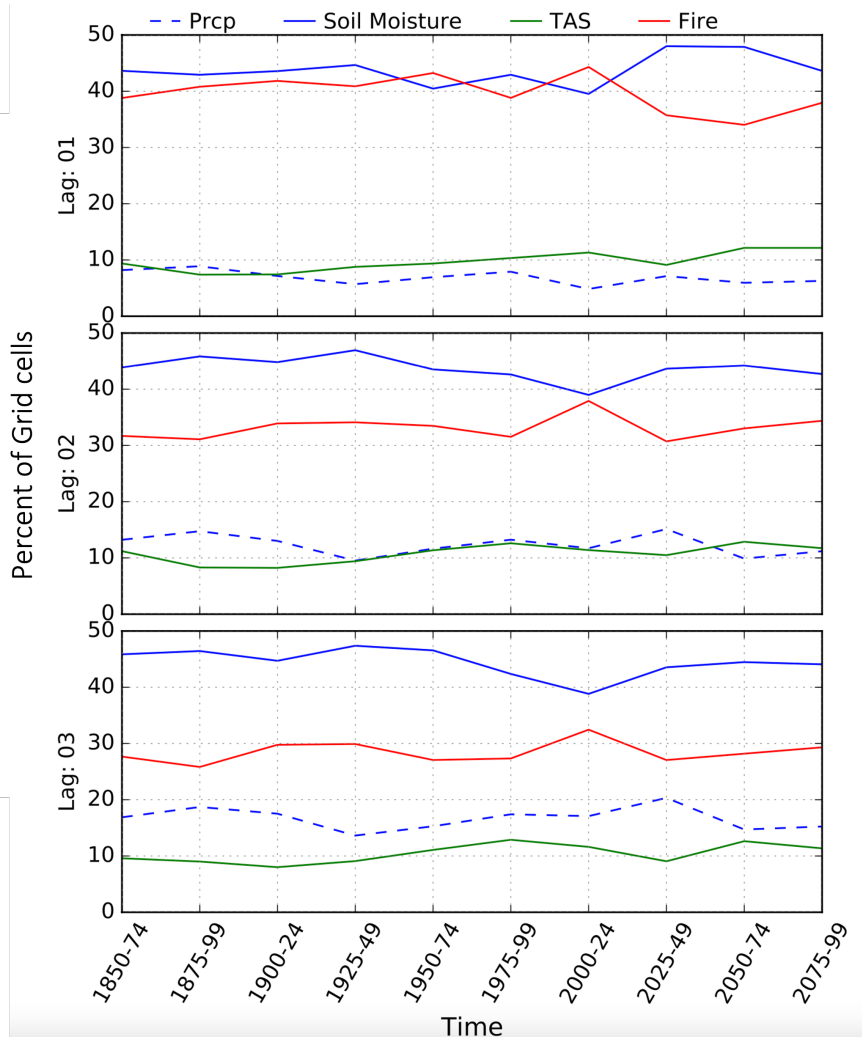


**Figure S6.** Percent distribution of number of grid cells with dominant climate drivers causing time continuous carbon cycle extremes from 1850 to 2100 for every 25 year period. The dominance of climate drivers is estimated by the absolute magnitude of correlation coefficient ( $p < 0.05$ ) at lags of 1 (top), 2 (middle), and 3 (bottom) months.

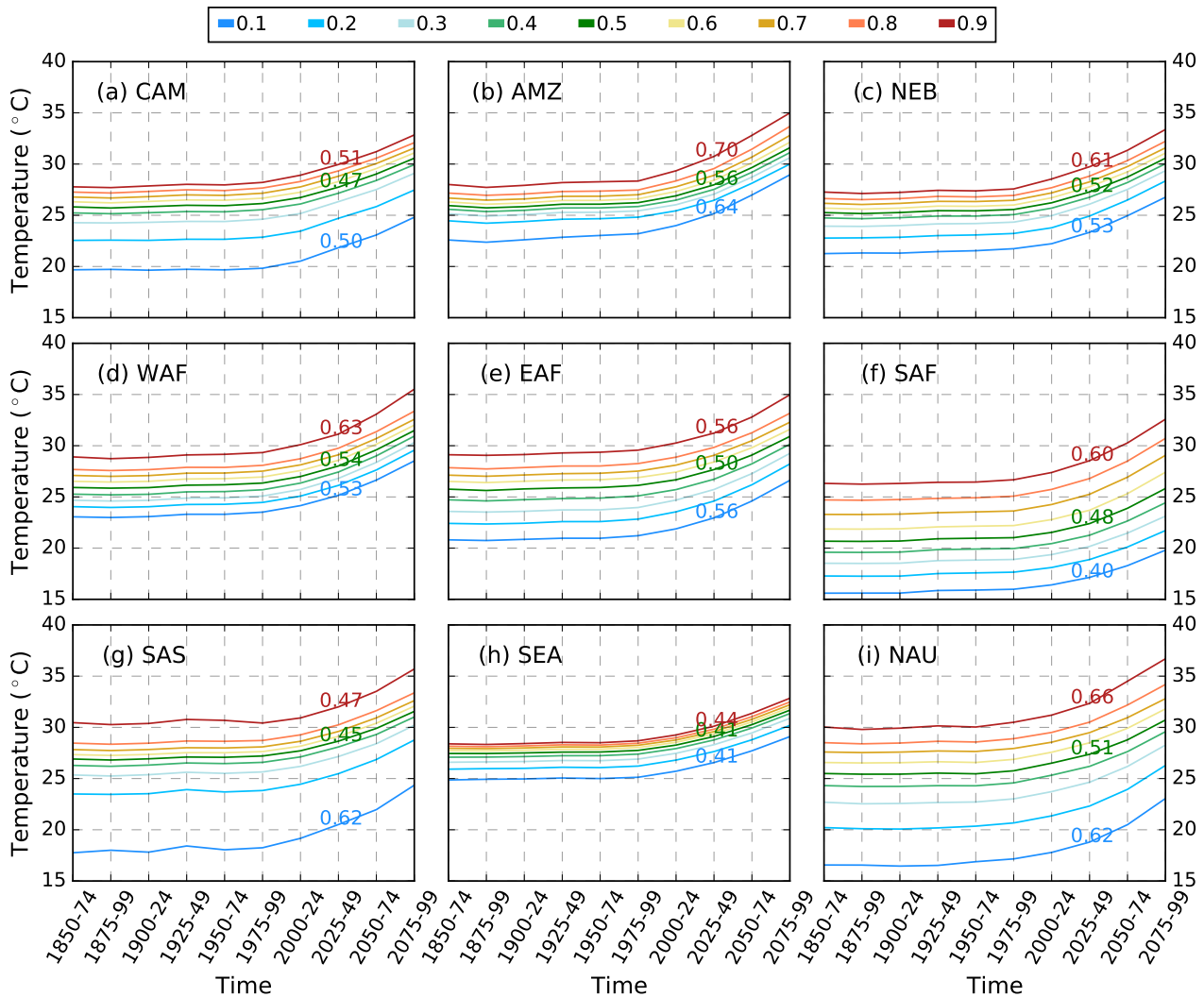


**Figure S7.** Change in area weighted average surface temperature (TAS) at various quantiles in the 9 SREX regions in tropics for 25 years windows from 1850 – 2100. The numbers shown in maroon, green, and blue in each subplot represent the rate of increase of temperature per decade ( $^{\circ}\text{C}/\text{decade}$ ) for 90<sup>th</sup>, median, and 10<sup>th</sup> quantile of temperatures, respectively.

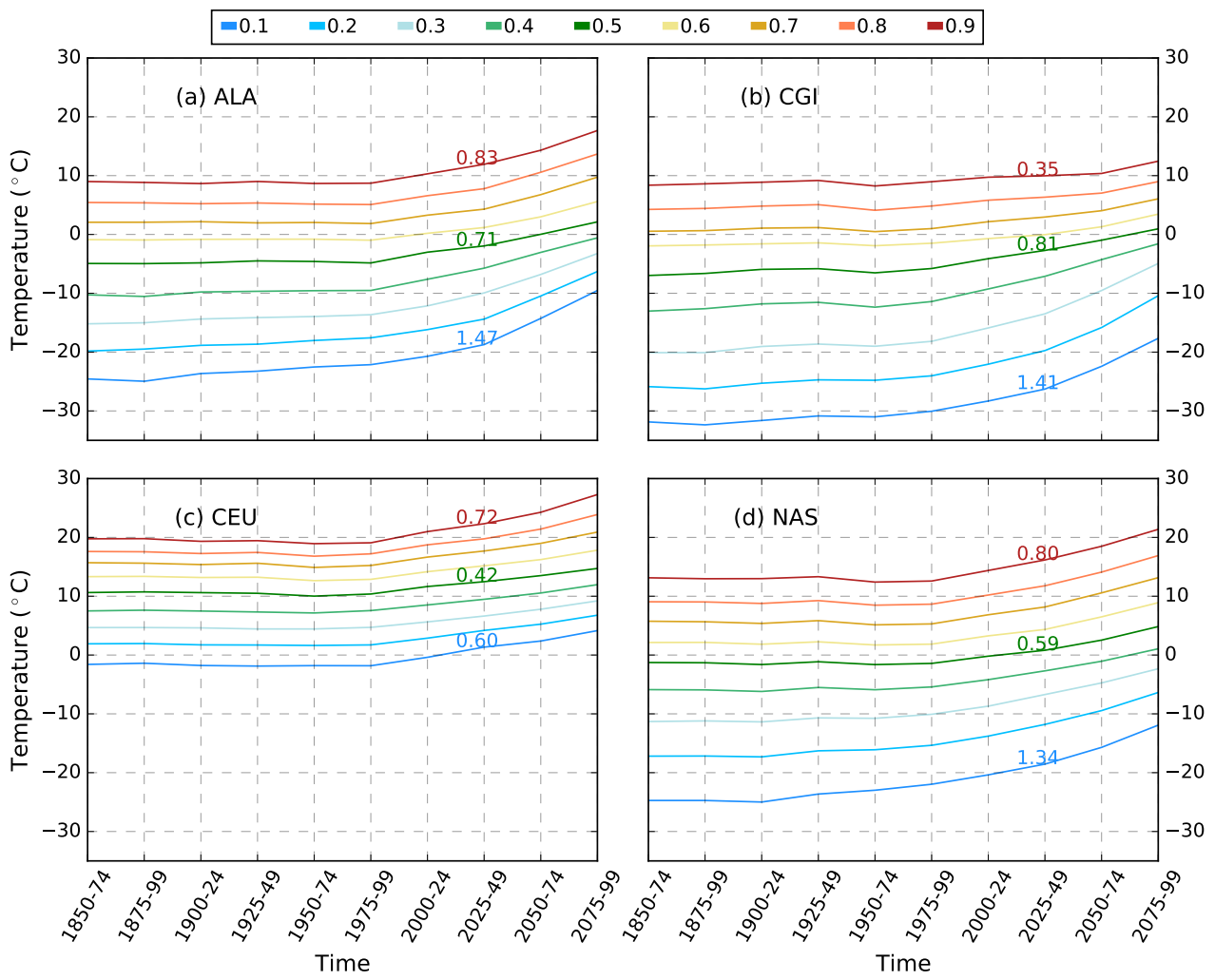


**Figure S8.** Change in area weighted average surface temperature (TAS) at various quantiles in the 9 SREX regions at high latitudes for 25 years windows from 1850–2100. The numbers shown in maroon, green, and blue in each subplot represent the rate of increase of temperature per decade ( $^{\circ}\text{C}/\text{decade}$ ) for 90<sup>th</sup>, median, and 10<sup>th</sup> quantile of temperatures, respectively.

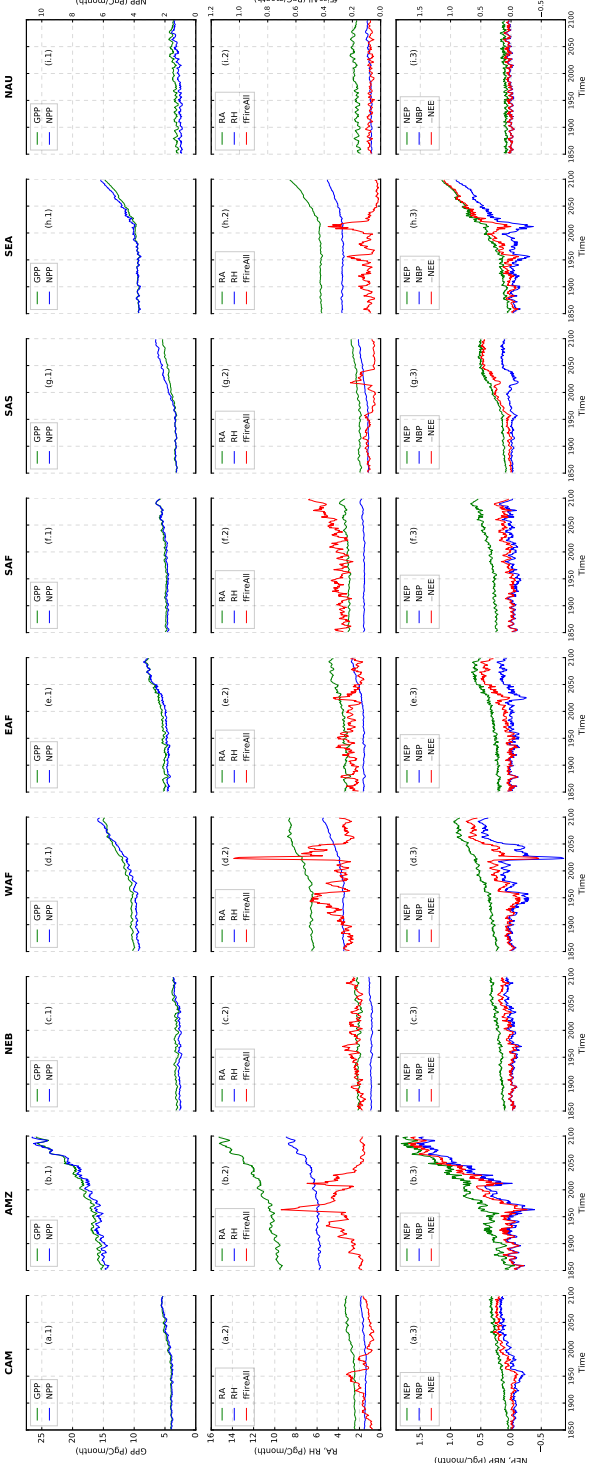


**Figure S9.** Timeseries of total carbon fluxes for the regions of (a) Central America/Mexico (CAM), (b) Amazon(AMZ), (c) North-East Brazil (NEB), (d) West Africa (WAF), (e) East Africa (EAF), (f) Southern Africa (SAF), (g) South Asia (SAS), (h) Southeast Asia (SEA), and (i) North Australia (NAU). Row 1 for each region shows the time series of total GPP (left y-axis) and NPP (right y-axis). Row 2 shows RA and RH on left y-axis and fFireAll on right y-axis. Row 3 shows NEP, NBP on left y-axis and –NEE on right y-axis. NEP is calculated by subtracting RH from NPP. NEP is surface net downward mass flux of carbon dioxide expressed as carbon due to all land processes excluding anthropogenic land use change. –NEE has the consistent direction with the carbon flux such as NBP and NPP.

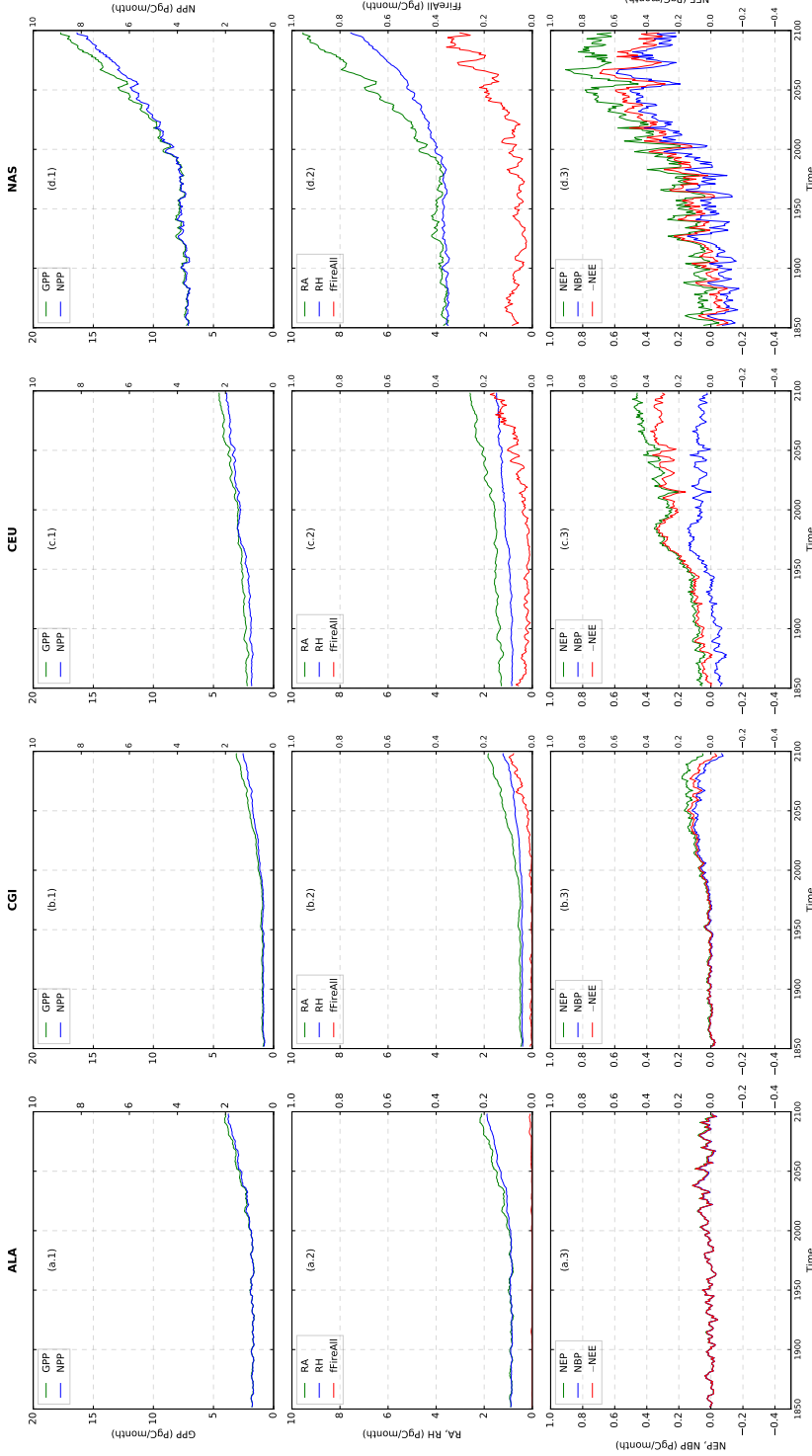


**Figure S10.** Timeseries of total carbon fluxes for the regions of (a) Alaska, (b) Canada, Greenland, and Iceland, (c) Central Europe, and (d) Northern Asia (NAS). Row 1 of every region shows the time series of total GPP (left y-axis) and NPP (right y-axis). Row 2 shows RA and RH on left y-axis and fFireAll on right y-axis. Row 3 shows NEP, NBP on left y-axis and -NEE on right y-axis. NEP is calculated by subtracting RH from NPP. NEP is surface net downward mass flux of carbon dioxide expressed as carbon due to all land processes excluding anthropogenic land use change. -NEE has the consistent direction with the carbon flux such as NBP and NPP.

*Author contributions.* BS designed the study with inputs from JK, FH, and AG. BS developed the statistical analysis methodology and codes, performed the data analysis, and wrote the manuscript with input from all co-authors.

405 *Competing interests.* The authors declare that they have no conflict of interest.

*Acknowledgements.* This research was supported by the Reducing Uncertainties in Biogeochemical Interactions through Synthesis and Computation (RUBISCO) Science Focus Area, which is sponsored by the Regional and Global Model Analysis (RGMA) activity of the Earth & Environmental Systems Modeling (EESM) Program in the Earth and Environmental Systems Sciences Division (EESSD) of the Office of Biological and Environmental Research (BER) in the US Department of Energy Office of Science. This research used resources of  
410 the National Energy Research Scientific Computing Center (NERSC), a U.S. Department of Energy Office of Science User Facility located at Lawrence Berkeley National Laboratory, operated under Contract No. DE-AC02-05CH11231 for the Project m2467.

We acknowledge the World Climate Research Programme, which, through its Working Group on Coupled Modelling, coordinated and promoted CMIP6. We thank the climate modeling groups for producing and making available their model output, the Earth System Grid Federation (ESGF) for archiving the data and providing access, and the multiple funding agencies who support CMIP6 and ESGF. We thank  
415 DOE's RGMA program area, the Data Management program, and NERSC for making this coordinated CMIP6 analysis activity possible.

## References

- Ault, T. R.: On the essentials of drought in a changing climate, *Science*, 368, 256–260, <https://doi.org/10.1126/science.aaz5492>, 2020.
- Bonan, G.: *Ecological Climatology: Concepts and Applications*, Cambridge University Press, 3 edn., <https://doi.org/10.1017/CBO9781107339200>, 2015.
- 420 Commane, R., Lindaas, J., Benmergui, J., Luus, K. A., Chang, R. Y.-W., Daube, B. C., Euskirchen, E. S., Henderson, J. M., Karion, A., Miller, J. B., Miller, S. M., Parazoo, N. C., Randerson, J. T., Sweeney, C., Tans, P., Thoning, K., Veraverbeke, S., Miller, C. E., and Wofsy, S. C.: Carbon dioxide sources from Alaska driven by increasing early winter respiration from Arctic tundra, *Proceedings of the National Academy of Sciences*, 114, 5361–5366, <https://doi.org/10.1073/pnas.1618567114>, 2017.
- Danabasoglu, G., Lamarque, J.-F., Bacmeister, J., Bailey, D. A., DuVivier, A. K., Edwards, J., Emmons, L. K., Fasullo, J., Garcia, R., Gettelman, A., Hannay, C., Holland, M. M., Large, W. G., Lauritzen, P. H., Lawrence, D. M., Lenaerts, J. T. M., Lindsay, K., Lipscomb, W. H., Mills, M. J., Neale, R., Oleson, K. W., Otto-Bliesner, B., Phillips, A. S., Sacks, W., Tilmes, S., van Kampenhout, L., Vertenstein, M., Bertini, A., Dennis, J., Deser, C., Fischer, C., Fox-Kemper, B., Kay, J. E., Kinnison, D., Kushner, P. J., Larson, V. E., Long, M. C., Mickelson, S., Moore, J. K., Nienhouse, E., Polvani, L., Rasch, P. J., and Strand, W. G.: The Community Earth System Model Version 2 (CESM2), *Journal of Advances in Modeling Earth Systems*, 12, e2019MS001916, <https://doi.org/10.1029/2019MS001916>, e2019MS001916 2019MS001916, 2020.
- 425 Diffenbaugh, N. S., Singh, D., Mankin, J. S., Horton, D. E., Swain, D. L., Touma, D., Charland, A., Liu, Y., Haugen, M., Tsiang, M., and Rajaratnam, B.: Quantifying the influence of global warming on unprecedented extreme climate events, *Proceedings of the National Academy of Sciences*, 114, 4881–4886, <https://doi.org/10.1073/pnas.1618082114>, 2017.
- Dormann, C. F., Elith, J., Bacher, S., Buchmann, C., Carl, G., Carré, G., Marquéz, J. R. G., Gruber, B., Lafourcade, B., Leitão, P. J., Münkemüller, T., McClean, C., Osborne, P. E., Reineking, B., Schröder, B., Skidmore, A. K., Zurell, D., and Lautenbach, S.: Collinearity: a review of methods to deal with it and a simulation study evaluating their performance, *Ecography*, 36, 27–46, <https://doi.org/https://doi.org/10.1111/j.1600-0587.2012.07348.x>, 2013.
- 430 Flach, M., Brenning, A., Gans, F., Reichstein, M., Sippel, S., and Mahecha, M. D.: Vegetation modulates the impact of climate extremes on gross primary production, *Biogeosciences Discussions*, 2020, 1–20, <https://doi.org/10.5194/bg-2020-80>, 2020.
- Frank, D., Reichstein, M., Bahn, M., Thonicke, K., Frank, D., Mahecha, M. D., Smith, P., van der Velde, M., Vicca, S., Babst, F., Beer, C., Buchmann, N., Canadell, J. G., Ciais, P., Cramer, W., Ibrom, A., Miglietta, F., Poulter, B., Rammig, A., Seneviratne, S. I., Walz, A., Wattenbach, M., Zavala, M. A., and Zscheischler, J.: Effects of climate extremes on the terrestrial carbon cycle: concepts, processes and potential future impacts, *Global Change Biology*, 21, 2861–2880, <https://doi.org/10.1111/gcb.12916>, 2015.
- 440 Friedlingstein, P., Jones, M., O'sullivan, M., Andrew, R., Hauck, J., Peters, G., Peters, W., Pongratz, J., Sitch, S., Le Quéré, C., et al.: Global carbon budget 2019, *Earth System Science Data*, 11, 1783–1838, 2019.
- Golyandina, N., Nekrutkin, V., and Zhigljavsky, A. A.: *Analysis of Time Series Structure: SSA and Related Techniques*, Chapman and Hall/CRC, 1 edn., <https://doi.org/https://doi.org/10.1201/9781420035841>, 2001.
- Grose, M. R., Narsey, S., Delage, F. P., Dowdy, A. J., Bador, M., Boschat, G., Chung, C., Kajtar, J. B., Rauniyar, S., Freund, M. B., Lyu, K., Rashid, H., Zhang, X., Wales, S., Trenham, C., Holbrook, N. J., Cowan, T., Alexander, L., Arblaster, J. M., and Power, S.: Insights 450 From CMIP6 for Australia's Future Climate, *Earth's Future*, 8, e2019EF001469, <https://doi.org/https://doi.org/10.1029/2019EF001469>, e2019EF001469 2019EF001469, 2020.

- Hubau, W., Lewis, S. L., Phillips, O. L., Affum-Baffoe, K., Beeckman, H., Cuní-Sánchez, A., Daniels, A. K., Ewango, C. E., Fauset, S., Mukinzi, J. M., et al.: Asynchronous carbon sink saturation in African and Amazonian tropical forests, *Nature*, 579, 80–87, <https://doi.org/10.1038/s41586-020-2035-0>, 2020.
- 455 Jones, M. H., Fahnstock, J. T., Walker, D. A., Walker, M. D., and Welker, J. M.: Carbon Dioxide Fluxes in Moist and Dry Arctic Tundra during the Snow-free Season: Responses to Increases in Summer Temperature and Winter Snow Accumulation, *Arctic and Alpine Research*, 30, 373–380, <https://doi.org/10.1080/00040851.1998.12002912>, 1998.
- Langenbrunner, B., Pritchard, M. S., Kooperman, G. J., and Randerson, J. T.: Why Does Amazon Precipitation Decrease When Tropical Forests Respond to Increasing CO<sub>2</sub>?, *Earth's Future*, 7, 450–468, <https://doi.org/10.1029/2018EF001026>, 2019.
- 460 Lawrence, D. M., Fisher, R. A., Koven, C. D., Oleson, K. W., Swenson, S. C., Bonan, G., Collier, N., Ghimire, B., van Kampenhout, L., Kennedy, D., et al.: The Community Land Model version 5: Description of new features, benchmarking, and impact of forcing uncertainty, *Journal of Advances in Modeling Earth Systems*, 11, 4245–4287, 2019.
- Li, F., Levis, S., and Ward, D. S.: Quantifying the role of fire in the Earth system; Part 1: Improved global fire modeling in the Community Earth System Model (CESM1), *Biogeosciences*, 10, 2293–2314, <https://doi.org/10.5194/bg-10-2293-2013>, 2013.
- 465 Liu, L., Gudmundsson, L., Hauser, M., Qin, D., Li, S., and Seneviratne, S. I.: Soil moisture dominates dryness stress on ecosystem production globally, *Nature Communications*, 11, 1–9, 2020.
- Marcolla, B., Migliavacca, M., Rödenbeck, C., and Cescatti, A.: Patterns and trends of the dominant environmental controls of net biome productivity, *Biogeosciences*, 17, 2365–2379, <https://doi.org/10.5194/bg-17-2365-2020>, 2020.
- Natali, S. M., Watts, J. D., Rogers, B. M., Potter, S., Ludwig, S. M., Selbmann, A.-K., Sullivan, P. F., Abbott, B. W., Arndt, K. A., 470 Birch, L., et al.: Large loss of CO<sub>2</sub> in winter observed across the northern permafrost region, *Nature Climate Change*, 9, 852–857, <https://doi.org/10.1038/s41558-019-0592-8>, 2019.
- Pan, S., Yang, J., Tian, H., Shi, H., Chang, J., Ciais, P., Francois, L., Frieler, K., Fu, B., Hickler, T., Ito, A., Nishina, K., Ostberg, S., Reyer, C. P., Schaphoff, S., Steinkamp, J., and Zhao, F.: Climate Extreme Versus Carbon Extreme: Responses of Terrestrial Carbon Fluxes to Temperature and Precipitation, *Journal of Geophysical Research: Biogeosciences*, 125, e2019JG005252, 475 <https://doi.org/10.1029/2019JG005252>, 2019.
- Piao, S., Sitch, S., Ciais, P., Friedlingstein, P., Peylin, P., Wang, X., Ahlström, A., Anav, A., Canadell, J. G., Cong, N., Huntingford, C., Jung, M., Levis, S., Levy, P. E., Li, J., Lin, X., Lomas, M. R., Lu, M., Luo, Y., Ma, Y., Myneni, R. B., Poulter, B., Sun, Z., Wang, T., Viovy, N., Zaehle, S., and Zeng, N.: Evaluation of terrestrial carbon cycle models for their response to climate variability and to CO<sub>2</sub> trends, *Global Change Biology*, 19, 2117–2132, <https://doi.org/10.1111/gcb.12187>, 2013.
- 480 Piao, S., Zhang, X., Chen, A., Liu, Q., Lian, X., Wang, X., Peng, S., and Wu, X.: The impacts of climate extremes on the terrestrial carbon cycle: A review, *Science China Earth Sciences*, 62, 1551–1563, 2019.
- Reichstein, M., Bahn, M., Ciais, P., Frank, D., Mahecha, M. D., Seneviratne, S. I., Zscheischler, J., Beer, C., Buchmann, N., Frank, D. C., Papale, D., Rammig, A., Smith, P., Thonicke, K., van der Velde, M., Vicca, S., Walz, A., and Wattenbach, M.: Climate extremes and the carbon cycle, *Nature*, 500, 287–295, <https://doi.org/10.1038/nature12350>, 2013.
- 485 Ribeiro, A. F. S., Russo, A., Gouveia, C. M., Páscoa, P., and Zscheischler, J.: Risk of crop failure due to compound dry and hot extremes estimated with nested copulas, *Biogeosciences*, 17, 4815–4830, <https://doi.org/10.5194/bg-17-4815-2020>, 2020.
- Seneviratne, S. I., Nicholls, N., Easterling, D., Goodess, C. M., Kanae, S., Kossin, J., Luo, Y., Marengo, J., McInnes, K., Rahimi, M., Reichstein, M., Sorteberg, A., Vera, C., and Zhang, X.: Changes in Climate Extremes and their Impacts on the Natural Physical Environment, pp. 109–230, Cambridge Univ. Press, Cambridge, U.K., and New York, [Field, C.B., V. Barros, T.F. Stocker, D. Qin, D.J. Dokken, K.L.

- 490 Ebi, M.D. Mastrandrea, K.J. Mach, G.-K. Plattner, S.K. Allen, M. Tignor, and P.M. Midgley (eds.)]. A Special Report of Working Groups I and II of the Intergovernmental Panel on Climate Change (IPCC), 2012.
- Sharma, B., Kumar, J., Collier, N., Ganguly, A. R., and Hoffman, F. M.: Quantifying Carbon Cycle Extremes and Attributing Their Causes Under Climate and Land Use and Land Cover Change From 1850 to 2300, *Journal of Geophysical Research: Biogeosciences*, 127, e2021JG006738, <https://doi.org/10.1029/2021JG006738> e2021JG006738 2021JG006738, 2022.
- 495 Turetsky, M. R., Abbott, B. W., Jones, M. C., Anthony, K. W., Olefeldt, D., Schuur, E. A., Grosse, G., Kuhry, P., Hugelius, G., Koven, C., et al.: Carbon release through abrupt permafrost thaw, *Nature Geoscience*, 13, 138–143, 2020.
- von Buttlar, J., Zscheischler, J., Rammig, A., Sippel, S., Reichstein, M., Knohl, A., Jung, M., Menzer, O., Arain, M. A., Buchmann, N., Cescatti, A., Gianelle, D., Kiely, G., Law, B. E., Magliulo, V., Margolis, H., McCaughey, H., Merbold, L., Migliavacca, M., Montagnani, L., Oechel, W., Pavelka, M., Peichl, M., Rambal, S., Raschi, A., Scott, R. L., Vaccari, F. P., van Gorsel, E., Varlagin, A., Wohlfahrt, G., 500 and Mahecha, M. D.: Impacts of droughts and extreme-temperature events on gross primary production and ecosystem respiration: a systematic assessment across ecosystems and climate zones, *Biogeosciences*, 15, 1293–1318, <https://doi.org/10.5194/bg-15-1293-2018>, 2018.
- Walker, A. P., De Kauwe, M. G., Medlyn, B. E., Zaehle, S., Iversen, C. M., Asao, S., Guenet, B., Harper, A., Hickler, T., Hungate, B. A., et al.: Decadal biomass increment in early secondary succession woody ecosystems is increased by CO<sub>2</sub> enrichment, *Nature Communications*, 505 10, 1–13, <https://doi.org/10.1038/s41467-019-08348-1>, 2019.
- Wu, Z., K. Schneider, E., Kirtman, B., Sarachik, E., Huang, N., and J. Tucker, C.: The modulated annual cycle: An alternative reference frame for climate anomalies, *Climate Dynamics*, 31, 823–841, <https://doi.org/10.1007/s00382-008-0437-z>, 2008.
- Zhang, T., Xu, M., Xi, Y., Zhu, J., Tian, L., Zhang, X., Wang, Y., Li, Y., Shi, P., Yu, G., Sun, X., and Zhang, Y.: Lagged climatic effects on carbon fluxes over three grassland ecosystems in China, *Journal of Plant Ecology*, 8, 291–302, <https://doi.org/10.1093/jpe/rtu026>, 2014.
- 510 Zscheischler, J., Mahecha, M. D., von Buttlar, J., Harmeling, S., Jung, M., Rammig, A., Randerson, J. T., Schölkopf, B., Seneviratne, S. I., Tomelleri, E., Zaehle, S., and Reichstein, M.: A few extreme events dominate global interannual variability in gross primary production, *Environmental Research Letters*, 9, 035 001, <https://doi.org/10.1088/1748-9326/9/3/035001>, 2014.
- Zscheischler, J., Westra, S., Van Den Hurk, B. J., Seneviratne, S. I., Ward, P. J., Pitman, A., Aghakouchak, A., Bresch, D. N., Leonard, M., Wahl, T., and Zhang, X.: Future climate risk from compound events, *Nature Climate Change*, 8, 469–477, <https://doi.org/10.1038/s41558-018-0156-3>, 2018.